Prepared for submission to JHEP DCPT-12/33

A chiral magnetic spiral in the holographic Sakai-Sugimoto model

Alfonso Ballon-Bayona, Kasper Peeters and Marija Zamaklar

Department of Mathematical Sciences,
Durham University,
South Road,
Durham DH1 3LE,
United Kingdom.
E-mail: c.a.m.ballonbayona@durham.ac.uk,
kasper.peeters@durham.ac.uk, marija.zamaklar@durham.ac.uk

Abstract: We investigate the effect of a magnetic field on the vacuum of low-temperature QCD at large-N_c in the presence of a chiral chemical potential, using the holographic Sakai-Sugimoto model. Above some critical chemical potential we find an instability, which triggers a decay of the homogeneous vacuum to a non-homogeneous configuration with a spiral form, which we construct explicitly. We find that this decay is suppressed for sufficiently large magnetic field, and determine the critical strength. We find that the new vacuum does not exhibit the chiral magnetic effect. This is related to the way the chiral chemical potential is introduced. We discuss an alternative way of introducing the chiral chemical potential that leads to a nonzero chiral magnetic effect.

Keywords: AdS/QCD, chemical potential, chiral magnetic spiral

Contents

1 Introduction and discussion

Recent work by various authors has provided evidence that in QCD, a magnetic field leads to several interesting phenomena, for values of the magnetic field which are substantially smaller than anticipated in earlier studies. The origin of these effects lies in the chiral axial anomaly and the additional couplings it provides. For instance, it has been shown [1] that the axial anomaly is responsible for the appearance of *pion domain walls*, which carry baryon charge. These are stable for sufficiently large baryon chemical potentials. Importantly, they form for relatively small critical values of the magnetic field, as this critical value scales with the pion mass.

In the presence of an axial chemical potential [2, 3], an external magnetic field can trigger the appearance of a vectorial current in the direction of this field,

$$\vec{j}_V \sim e\mu_A \vec{B}\,. \tag{1.1}$$

The origin of this so called *chiral magnetic effect* (CME) is the asymmetry between left- and right-handed fermions (parametrised by the axial potential μ_A), which leads to separation of electric charge. Related to this is the *chiral separation effect* [4–6], where instead of an axial potential, a baryonic quark potential is introduced. The magnetic field now leads to a separation of chiral charge, and an *axial* current is generated,

$$\vec{j}_A \sim e\mu_B \vec{B}\,. \tag{1.2}$$

Combining these two effects leads to evidence for the existence of a so-called *chiral magnetic wave* [7]. All these effects suggest that the consequence of a magnetic field may be much more important (and potentially easier to see in experiments) than previously thought.

These effects were originally derived using a quasi-particle picture of chiral charge carriers, which is only valid at weak coupling. They have meanwhile also been confirmed in a number of holographic descriptions of the strong coupling regime. The pion gradient walls were found in the Sakai-Sugimoto model in [8, 9] (see also [10]), and there are even abelian analogues of this solution [11] which involve an η'-meson gradient (and of course no baryon number in this case). Whether or not holographic models exhibit the CME or CSE is subject of more controversy, as it requires a careful definition of the holographic currents. An analysis of the D3/D7 system was given in [12, 13] and we will comment extensively on the Sakai-Sugimoto model later in this paper.

A major question is what happens when the chemical potentials are large enough so that they trigger a condensation of bound states. Even without a magnetic field and without an axial anomaly, various models predict the formation of a non-isotropic (although homogeneous) vector meson condensate, once the axial chemical potential becomes of the order of the meson mass (see [14] for an analysis in the Sakai-Sugimoto model relevant here, and a list of references to other works). When the axial anomaly is present, the condensate is typically no longer even homogeneous, but forms a spiral structure [15]. A lot of work in this direction focuses on high temperature models, but in fact such condensation already happens at low and zero temperatures [14, 15].

In the present paper, we therefore examine the Sakai-Sugimoto model in the presence of a magnetic field and an abelian chiral chemical potential, and set out to determine whether there is an instability against decay to a non-homogeneous chiral spiral also in this case. We will also analyse whether the ground state exhibits a chiral magnetic effect, and whether there is an η'-gradient in this case. We will only

consider the confined chirally broken phase of this model, i.e. the low-temperature behaviour.

Our main results are as follows. First, we determine the location of the phase boundary between the homogeneous solution of [8, 9] and a new chiral spiral like solution[1]. We construct the non-homogeneous chiral spiral like solution explicitly.[2] We establish that the latter still does not exhibit the CME, but point out that this conclusion relies crucially on subtleties related to the precise way in which the chemical potential is introduced. Finally, we show that a magnetic field tends to stabilise the homogeneous solution, and there is a critical value beyond which the chiral spiral ceases to exist. The parameter space in which we need to scan for non-linear spiral solutions is rather large and the numerical analysis is consequently sometimes tricky; we comment on details of this procedure in the appendix.

An important issue in this analysis is the precise way in which the chemical potential is included in the holographic setup. It was recently pointed out [13, 16] that the usual approach, which roughly amounts to identifying the chemical potential with the asymptotic value of the gauge field, may be incorrect in case the associated charge is not conserved (like, in our case, the axial charge). However, we can define μ_A as the integrated radial electric flux between the two boundaries of the brane. Following the field theory arguments of [16] we will argue that there are then two natural formalisms for introducing the chemical potential. In formalism A we introduce μ_A through boundary conditions in the component $\mathcal{A}_0$ of the gauge field. In formalism B the chemical potential instead sits in $\mathcal{A}_z$. In the presence of the axial anomaly these two formalisms are inequivalent.

In formalism A, we find that the non-homogeneous phase characterised by wave number k, is dominant and there is a preferred value of this wave number $k = k_{\text{g.s.}}$. When the magnetic field is small compared to the chiral chemical potential $B \ll \mu_A$, $k_{\text{g.s.}}$ depends only very weakly on the value of μ_A. This result is consistent with our previous work [15]. For sufficiently large magnetic field we find that the non-homogeneous ground state is suppressed. In formalism B, on the other hand, the homogeneous state always has lower energy than the non-homogeneous one, and there is hence no chiral magnetic spiral.

As far as the chiral magnetic effect is concerned, we find that in formalism A the effect is absent. This result is consistent with previous calculations on the Sakai-Sugimoto model [17]. In formalism B, on the other hand, there exists a non-zero chiral magnetic effect. This seems to be more in line with recent lattice calculations [18],

[1] The stability analysis of the homogeneous solution presented in [11] is incorrect in some crucial aspects; we will comment on the details and the consequences later.

[2] The chiral magnetic wave mentioned earlier is different from the chiral magnetic spiral, because the chiral magnetic wave involves the density and the component of the current parallel to the magnetic field, while the chiral magnetic spiral involves the components of the current transverse to the magnetic field.

chiral model calculations [19] and holographic bottom-up models [20, 21] for the confined chirally broken phase of QCD. However, a main shortcoming of formalism B is that the inhomogeneous phase, whose existence is indicated by our perturbative analysis, is absent in the full nonlinear theory. Since the perturbative analysis is blind to the subtle issues on how one introduces the chemical potential in the holographic setup, we are inclined to think that, as it stands, formalism B is incorrect. Whether formalism A is correct on the other hand, or also needs to be altered, is an open question at the moment, and needs a separate study, which we leave for future work.

2 Chemical potentials, currents and anomalies

2.1 Effective five-dimensional action

In order to set the scene and to introduce our conventions, let us start by giving a brief review of the basics of the Sakai-Sugimoto model [22, 23]. For a more detailed description of the features of this model which are relevant here, we refer the reader to the original papers or to [15].

The Sakai-Sugimoto model at low temperature consists of N_f flavour D8-branes and N_f anti-D8-branes which are placed in the gravitational background sourced by a large number N_c of D4-branes which are compactified on a circle of radius R. In the simplest set up, the probes are asymptotically positioned at the antipodal points of a circle, while in the interior of the geometry they merge together into one U-shaped object. The gauge theory on the world-volume of the probe brane is nine-dimensional, containing a four-dimensional sphere, the holographic direction and four directions parallel to the boundary. By focusing on the sector of the theory that does not include excitations over the S^4, one can integrate the probe brane action over this sub-manifold and end up with an effective five dimensional DBI action on the probe brane world-volume. By expanding this action to the leading order in the string tension, one ends up with a five dimensional Yang-Mills theory with a Chern-Simons term. For $N_f = 1$ we can write the action as

$$S = S_{\rm YM} + S_{\rm CS} = -\frac{\kappa}{2}\int {\rm d}^4x{\rm d}z\sqrt{-g}\,\mathcal{F}^{mn}\mathcal{F}_{mn} + \frac{\alpha}{4}\,\epsilon^{\ell mnpq}\int {\rm d}^4x{\rm d}z\mathcal{A}_\ell\mathcal{F}_{mn}\mathcal{F}_{pq}\,. \quad (2.1)$$

where the indices are now raised or lowered using the effective five dimensional metric g_{mn}. This metric is defined as

$${\rm d}s^2_{(5)} = g_{mn}{\rm d}x^m{\rm d}x^n = M^2_{\rm KK}K_z^{2/3}\,\eta_{\mu\nu}{\rm d}x^\mu{\rm d}x^\nu \,+\, K_z^{-2/3}{\rm d}z^2\,, \quad (2.2)$$

where $K_z \equiv (1+z^2)$. The x^μ directions are parallel to the boundary and z is the holographic direction orthogonal to the boundary. The coupling constants κ and α are given in terms of the number of colours N_c, the compactification mass scale $M_{\rm KK}$ and the 't Hooft coupling λ by

$$\kappa = \frac{\sqrt{\alpha'}g_sN_c^2M_{\rm KK}}{108\pi^2} = \frac{\lambda N_c}{216\pi^3}\,, \qquad \alpha = \frac{N_c}{24\pi^2}\,. \quad (2.3)$$

The Chern-Simons term written in (2.1) is valid only for a single D8 probe, i.e. for a $U(1)$ gauge theory on the brane world-volume.

2.2 Symmetries and chemical potentials

Holographic models encode *global* symmetries of the dual gauge theory in the form of *gauge* symmetries in the bulk theory, and these relations hold both for the closed as well as the open sectors of the string theory. The same is true for the Sakai-Sugimoto model at hand, where there are two independent gauge theories living near the two boundaries of the flavour D8-$\overline{\text{D8}}$ brane system. These $U(N_f)_L$ and $U(N_f)_R$ gauge symmetries correspond to the global $U(N_f) \times U(N_f)_R$ flavour symmetries of the dual gauge theory. In the low-temperature phase of the Sakai-Sugimoto model that we are interested in, the two branes are connected in the interior of the bulk space, and thus the gauge fields $\mathcal{A}_M^L$ and $\mathcal{A}_M^R$ are limits of a single gauge field living on the two connected branes. Therefore, one cannot independently perform gauge transformations on these two gauge fields, but is constrained to gauge transformations which, as $z \to \pm\infty$, act in a related way. Specifically, since near the boundary a large bulk gauge transformation acts as $\mathcal{A}_{L/R} \to g_{L/R}\mathcal{A}_{L/R}g_{L/R}^{-1}$, then clearly any state (and in particular the trivial vacuum $\mathcal{A} = 0$) is invariant under the vectorial transformations, i.e. those transformations for which $g_L = g_R$. This means that the vector-like symmetry is unbroken in this model. On the other hand, the fact that the branes are joined into one U-shaped object means that the axial symmetry is broken, which corresponds to the *spontaneous* breaking of the axial symmetry in the dual gauge theory. The corresponding Goldstone bosons can be seen explicitly in the spectrum of the fluctuations on the brane world-volume.

The relationship between the bulk gauge field and the source and global symmetry current of the dual gauge theory is encoded in the asymptotic behaviour of the former. More precisely, the bulk gauge field $\mathcal{A}_M(z, x^\mu)$ behaves, near the boundary and in the $\mathcal{A}_z = 0$ gauge, as

$$\mathcal{A}_\nu(x^\mu, z) \to a_\nu(x^\mu)\Big(1 + \mathcal{O}(z^{-2/3})\Big) + \rho_\nu(x^\mu)\frac{1}{z}\Big(1 + \mathcal{O}(z^{-2/3})\Big)\,. \tag{2.4}$$

Here ρ_ν parametrises the normalisable mode, while $a_\nu(x^\mu)$ describes the non-normalisable behaviour of the field. The latter is interpreted as a source in the dual field theory action, where it appears as

$$\int \mathrm{d}^4x\, a_\nu(x^\mu)J^\nu(x^\mu)\,. \tag{2.5}$$

Hence the expectation value of the current corresponding to the global symmetry in the gauge theory is given by

$$J^\mu(x)_\pm = \frac{\delta S}{\delta A_\mu(x, z \to \pm\infty)}\,. \tag{2.6}$$

When the bulk action is just the ordinary Yang-Mills action (in curved space), this expectation value is the same as the coefficient ρ_ν in the expansion (2.4). However, in the presence of the Chern-Simons term, the coefficient ρ_ν is different from the current, as we will explicitly demonstrate for the system at hand in section 2.3. This difference has been a source of some of confusion in the literature. Its importance has recently been emphasised in the context of the chiral magnetic effect in the Sakai-Sugimoto model in [24].

From (2.5) we also see that adding a chemical potential to the field theory corresponds to adding a source for J^0, which implies the boundary condition for the holographic gauge field $\mathcal{A}_\nu(x) = \mu\delta_{\nu 0}$.

For the Sakai-Sugimoto model, the bulk field $\mathcal{A}_m$ living on the D8-branes has *two* asymptotic regions, corresponding to each brane, and hence there are two independent chemical potentials μ_L and μ_R which can be separately turned on. Instead of left and right chemical potentials one often introduces vectorial and axial potentials, defined respectively as $\mu_B = \frac{1}{2}(\mu_R + \mu_L)$ and $\mu_A = \frac{1}{2}(\mu_R - \mu_L)$. For the $N_f = 2$ case, the vectorial and axial chemical potentials for the $U(1)$ subgroup of the $U(2)$ gauge group on the two D8-branes correspond to the baryonic and axial chemical potential in the dual gauge theory, while the non-abelian $SU(2)$ chemical potentials are mapped to the vectorial and axial isospin potentials.

In what follows we will also be interested in studying the system in the presence of an *external* (non-dynamical) magnetic source, which will be introduced by turning on a nontrivial profile for the non-normalisable component $a_\nu(x)$ of the bulk field.

2.3 The Chern-Simons term, anomalies and the Bardeen counter term

The symmetries and currents of the model discussed in the previous section are, however, valid only at leading order in λ^{-1}. At the next order in λ^{-1}, the Yang-Mills action on the brane world-volume receives many corrections, among which the Chern-Simons term. This term turns out to be crucial for the existence of a nontrivial ground state of the system in the presence of the external magnetic field, a situation which we will study in the following sections. On manifolds with boundaries, however, the Chern-Simons term is manifestly gauge non-invariant and it also spoils conservation of the vectorial and axial currents. Both of these reflect the fact that the Chern-Simons term is the holographic manifestation of the vector and axial gauge anomalies in the dual theory.

Apart from the Chern-Simons term there are of course also various other corrections. One important class of terms is coming from the expansion of the DBI action. In previous work [15] we have seen that the qualitative picture of chiral spiral formation at vanishing magnetic field does not change when these corrections are taken into account. We will assume that this holds true here as well. For the other higher derivative corrections, it is important to note that we will find that our ground state

has a momentum scale of order $M_{\rm KK}$, not $1/l_s$, so higher derivatives can typically be ignored as long as $M_{\rm KK} l_s$ is small.

Returning to the role of the Chern-Simons term in describing anomalies, let us start by decomposing the gauge field in terms of the axial and vectorial components, as

$$\mathcal{A}_m(x,z) = \mathcal{A}^V_m(x,z) + \mathcal{A}^A_m(x,z)\,. \tag{2.7}$$

These two components transform under under an inversion of the holographic coordinate $z \to -z$ as

$$\mathcal{A}^{V/A}_\mu(-z,x) = \pm\mathcal{A}^{V/A}_\mu(z,x)\,, \quad \mathcal{A}^{V/A}_z(-z,x) = \mp\mathcal{A}^{V/A}_z(z,x)\,. \tag{2.8}$$

Furthermore, the μ component of these fields are related to the dual gauge fields as

$$\mathcal{A}^V_\mu(z=\pm\infty,x) = A^V_\mu(x) \quad , \quad \mathcal{A}^A_\mu(z=\pm\infty,x) = \mp A^A_\mu(x)\,, \tag{2.9}$$

where the non-calligraphic $A^{V/A}_\mu(x)$ are the boundary vector and axial-vector gauge fields. When written in terms of these vectorial and axial potentials the action reads

$$\begin{aligned} S = \int \mathrm{d}^4x\mathrm{d}z\Big\{ &-\frac{\kappa}{2}\sqrt{-g}\left[\mathcal{F}^{mn}_V\mathcal{F}^V_{mn} + \mathcal{F}^{mn}_A\mathcal{F}^A_{mn}\right] \\ &+\frac{\alpha}{4}\epsilon^{\ell mnpq}\left[2\mathcal{A}^V_\ell\mathcal{F}^A_{mn}\mathcal{F}^V_{pq} + \mathcal{A}^A_\ell(\mathcal{F}^V_{mn}\mathcal{F}^V_{pq} + \mathcal{F}^A_{mn}\mathcal{F}^A_{pq})\right]\Big\}\,. \end{aligned} \tag{2.10}$$

We now want to compute the currents following the prescription (2.6). The variation of the action can be written as

$$\begin{aligned} \delta S = \int \mathrm{d}^4x\mathrm{d}z\Big\{ &\left[\frac{\partial\mathcal{L}}{\partial\mathcal{A}^V_\ell} - \partial_m\mathcal{P}^{m\ell}_V\right]\delta\mathcal{A}^V_\ell + \left[\frac{\partial\mathcal{L}}{\partial\mathcal{A}^A_\ell} - \partial_m\mathcal{P}^{m\ell}_A\right]\delta\mathcal{A}^A_\ell \\ &+\partial_m\left[\mathcal{P}^{m\ell}_V\delta\mathcal{A}^V_\ell + \mathcal{P}^{m\ell}_A\delta\mathcal{A}^A_\ell\right]\Big\}\,, \end{aligned} \tag{2.11}$$

where the derivatives of the Lagrangian are given by

$$\begin{aligned} \frac{\partial\mathcal{L}}{\partial\mathcal{A}^V_\ell} &= \frac{\alpha}{2}\epsilon^{\ell mnpq}\mathcal{F}^A_{mn}\mathcal{F}^V_{pq}\,, \\ \frac{\partial\mathcal{L}}{\partial\mathcal{A}^A_\ell} &= \frac{\alpha}{4}\epsilon^{\ell mnpq}(\mathcal{F}^V_{mn}\mathcal{F}^V_{pq} + \mathcal{F}^A_{mn}\mathcal{F}^A_{pq})\,, \\ \mathcal{P}^{m\ell}_V \equiv \frac{\partial\mathcal{L}}{\partial(\partial_m\mathcal{A}^V_\ell)} &= -2\kappa\sqrt{-g}\mathcal{F}^{m\ell}_V + \alpha\epsilon^{m\ell npq}(\mathcal{A}^V_n\mathcal{F}^A_{pq} + \mathcal{A}^A_n\mathcal{F}^V_{pq})\,, \\ \mathcal{P}^{m\ell}_A \equiv \frac{\partial\mathcal{L}}{\partial(\partial_m\mathcal{A}^A_\ell)} &= -2\kappa\sqrt{-g}\mathcal{F}^{m\ell}_A + \alpha\epsilon^{m\ell npq}(\mathcal{A}^V_n\mathcal{F}^V_{pq} + \mathcal{A}^A_n\mathcal{F}^A_{pq})\,. \end{aligned} \tag{2.12}$$

Note that $\mathcal{P}^{m\ell}_{V/A}$ are antisymmetric in $m \leftrightarrow \ell$. Imposing that the bulk term in the variation (the first line in (2.11)) vanishes gives the equations of motion,

$$\begin{aligned} 2\kappa\partial_m(\sqrt{-g}\mathcal{F}_V^{m\ell}) + \frac{3}{2}\alpha\epsilon^{\ell mnpq}\mathcal{F}^A_{mn}\mathcal{F}^V_{pq} = 0\,, \\ 2\kappa\partial_m(\sqrt{-g}\mathcal{F}_A^{m\ell}) + \frac{3}{4}\alpha\epsilon^{\ell mnpq}(\mathcal{F}^V_{mn}\mathcal{F}^V_{pq} + \mathcal{F}^A_{mn}\mathcal{F}^A_{pq}) = 0\,. \end{aligned} \tag{2.13}$$

We will need these shortly to show that the currents are not conserved. The boundary term in the action variation can be written as

$$\delta S_{\rm bdy} = \int \mathrm{d}^4x\mathrm{d}z \left\{\partial_z\left[\mathcal{P}_V^{z\mu}\delta\mathcal{A}^V_\mu + \mathcal{P}_A^{z\mu}\delta\mathcal{A}^A_\mu\right] + \partial_\mu\left[\mathcal{P}_V^{\mu\ell}\delta\mathcal{A}^V_\ell + \mathcal{P}_A^{\mu\ell}\delta\mathcal{A}^A_\ell\right]\right\}. \tag{2.14}$$

This implies that the holographic vector and axial currents are given by the expressions

$$\begin{aligned} J^\mu_V(x) &= -4\kappa\lim_{z\to\infty}\left[\sqrt{-g}\mathcal{F}_V^{z\mu}\right] - 2\alpha\epsilon^{\mu\nu\rho\sigma}(A^V_\nu F^A_{\rho\sigma} + A^A_\nu F^V_{\rho\sigma})\,, \\ J^\mu_A(x) &= 4\kappa\lim_{z\to\infty}\left[\sqrt{-g}\mathcal{F}_A^{z\mu}\right] - 2\alpha\epsilon^{\mu\nu\rho\sigma}(A^V_\nu F^V_{\rho\sigma} + A^A_\nu F^A_{\rho\sigma})\,, \end{aligned} \tag{2.15}$$

where we have used the boundary conditions (2.9) and $F^{V/A}_{\mu\nu} = \partial_\mu A^{V/A}_\nu - \partial_\nu A^{V/A}_\mu$ are the boundary field strengths.

Using the equations of motion (2.13) we can explicitly show that these two currents are not conserved due to the presence of the Chern-Simons term. One finds

$$\begin{aligned} \partial_\mu J^\mu_V(x) &= 2\lim_{z\to\infty}\partial_\mu\left[\sqrt{-g}\mathcal{P}_V^{z\mu}\right] \equiv -2\lim_{z\to\infty}\left[\sqrt{-g}\frac{\partial\mathcal{L}}{\partial\mathcal{A}^V_z}\right] \\ &= -\alpha\,\epsilon^{\mu\nu\rho\sigma}F^A_{\mu\nu}F^V_{\rho\sigma}\,, \\ \partial_\mu J^\mu_A(x) &= -2\lim_{z\to\infty}\partial_\mu\left[\sqrt{-g}\mathcal{P}_V^{z\mu}\right] \equiv 2\lim_{z\to\infty}\left[\sqrt{-g}\frac{\partial\mathcal{L}}{\partial\mathcal{A}^A_z}\right] \\ &= \frac{\alpha}{2}\,\epsilon^{\mu\nu\rho\sigma}(F^V_{\mu\nu}F^V_{\rho\sigma} + F^A_{\mu\nu}F^A_{\rho\sigma})\,, \end{aligned} \tag{2.16}$$

We see two things here. Firstly, the anomaly (i.e. the right-hand side of above equations) is indeed sourced by the Chern-Simons term. Secondly, the anomaly is present only if the *boundary* value of the bulk gauge *field strength* is non-vanishing. In other words, only in the presence of an *external* field does the anomaly show up.

While the axial anomaly is not problematic (it just reflects the fact that this symmetry is no longer present in the dual quantum field theory), this is not the case with the vectorial symmetry. In QED coupled to chiral fermions one has to require that the vector current is strictly conserved, since its non-conservation would imply a gauge anomaly. It is possible to make the vectorial current conserved by adding extra boundary terms to the action, as was first shown by Bardeen in [25].

In the holographic setup, one expects that such a Bardeen-type counter term will appear, but this type of term should come from the requirement that the full theory

in the bulk *in the presence of the boundary* is gauge invariant under vectorial gauge transformations. Let us therefore consider a generic *vectorial* gauge transformation in the bulk

$$\delta\mathcal{A}^V_\ell = \partial_\ell \Lambda_V(x,z)\,, \quad \delta\mathcal{A}^A_\ell = 0\,, \tag{2.17}$$

where $\Lambda_V(x,z)$ is a function even in z. Under this transformation, the action (2.10) is invariant up to a boundary term,

$$\begin{aligned}
\delta S^{(\Lambda_V)}_{\rm bdy} &= \int \mathrm{d}^4x\mathrm{d}z(\partial_\ell\Lambda_V)\partial_m\mathcal{P}^{m\ell}_V \\
&= \frac{\alpha}{2}\epsilon^{\ell mnpq}\int \mathrm{d}^4x\mathrm{d}z(\partial_\ell\Lambda_V)\mathcal{F}^A_{mn}\mathcal{F}^V_{pq} \\
&= \alpha\epsilon^{\ell mnpq}\int \mathrm{d}^4x\mathrm{d}z\partial_m\left[(\partial_\ell\Lambda_V)\mathcal{A}^A_n\mathcal{F}^V_{pq}\right]\,.
\end{aligned} \tag{2.18}$$

Therefore, if we want to impose invariance of the action under (2.17) we need to add the anomaly counter term correction

$$\begin{aligned}
S_{\rm an.} &= -\alpha\epsilon^{\ell mnpq}\int \mathrm{d}^4x\mathrm{d}z\partial_m\left[\mathcal{A}^V_\ell\mathcal{A}^A_n\mathcal{F}^V_{pq}\right] \\
&= \frac{\alpha}{2}\epsilon^{\ell mnpq}\int \mathrm{d}^4x\mathrm{d}z\left[-\mathcal{A}^V_\ell\mathcal{F}^A_{mn}\mathcal{F}^V_{pq} + \mathcal{A}^A_\ell\mathcal{F}^V_{mn}\mathcal{F}^V_{pq}\right]\,.
\end{aligned} \tag{2.19}$$

We see that there are two contributions of this surface term: at the "holographic" boundaries $z\to\pm\infty$ and at the boundary at spatial infinity $|\vec{x}|\to\infty$. Its contribution at holographic infinity is indeed the Bardeen counter term as derived in quantum field theory [25], and which was, in the holographic setup, initially postulated (added by hand) in [24]. We see that its presence automatically follows from the requirement of classical gauge invariance of the bulk theory in the presence of the boundary.

The contribution at spatial infinity, would typically vanish, as all physical states in the system are localised in the interior. However, in the presence of external sources which generate an external magnetic field that fills out the whole four-dimensional space, like the one we will be considering, it is not a priori clear if this is true, and one has to be careful about possible extra contributions to the action and currents. It will however turn out that for our non-homogeneous ansatz, these extra terms are irrelevant and that only the Bardeen counter term is non-vanishing.

Let us continue by showing the effect of adding the $S_{\rm an.}$ term on the currents. The total action now reads

$$\begin{aligned}
\tilde{S} = S + S_{\rm an.} = \int \mathrm{d}^4x\mathrm{d}z\Big\{ &-\frac{\kappa}{2}\sqrt{-g}\left[\mathcal{F}^{mn}_V\mathcal{F}^V_{mn} + \mathcal{F}^{mn}_A\mathcal{F}^A_{mn}\right] \\
&+ \frac{\alpha}{4}\epsilon^{\ell mnpq}\mathcal{A}^A_\ell(\,3\,\mathcal{F}^V_{mn}\mathcal{F}^V_{pq} + \mathcal{F}^A_{mn}\mathcal{F}^A_{pq})\Big\} \equiv \int \mathrm{d}^4x\mathrm{d}z\tilde{\mathcal{L}}\,.
\end{aligned} \tag{2.20}$$

The variation of this new action can again be written in the form (2.11), with $\tilde{\mathcal{L}}$ and $\tilde{P}$, instead of $\mathcal{L}$ and P, i.e.

$$\begin{aligned}
\frac{\partial\tilde{\mathcal{L}}}{\partial\mathcal{A}^V_\ell} &= 0\,,\\
\frac{\partial\tilde{\mathcal{L}}}{\partial\mathcal{A}^A_\ell} &= \frac{\alpha}{4}\epsilon^{\ell mnpq}(\,3\,\mathcal{F}^V_{mn}\mathcal{F}^V_{pq}+\mathcal{F}^A_{mn}\mathcal{F}^A_{pq})\,,\\
\tilde{P}^{m\ell}_V &\equiv \frac{\partial\tilde{\mathcal{L}}}{\partial(\partial_m\mathcal{A}^V_\ell)} = -2\kappa\sqrt{-g}\mathcal{F}^{m\ell}_V+3\alpha\epsilon^{m\ell npq}\mathcal{A}^A_n\mathcal{F}^V_{pq}\,,\\
\tilde{P}^{m\ell}_A &\equiv \frac{\partial\tilde{\mathcal{L}}}{\partial(\partial_m\mathcal{A}^A_\ell)} = -2\kappa\sqrt{-g}\mathcal{F}^{m\ell}_A+\alpha\epsilon^{m\ell npq}\mathcal{A}^A_n\mathcal{F}^A_{pq}\,.
\end{aligned} \tag{2.21}$$

The equations of motion are of course unchanged (as the Bardeen counter term is only a surface term), while the new currents are obtained as

$$\tilde{J}^\mu_{V/A}(x) = \frac{\delta\tilde{S}}{\delta A^{V/A}_\mu(x)} = \pm\frac{\delta\tilde{S}}{\delta\mathcal{A}^{V/A}_\mu(x,z=\infty)} = \pm 2\lim_{z\to\infty}\tilde{\mathcal{P}}^{z\mu}_{V/A}\,. \tag{2.22}$$

Explicitly, the expressions read

$$\begin{aligned}
\tilde{J}^\mu_V(x) &= -4\kappa\lim_{z\to\infty}\left[\sqrt{-g}\mathcal{F}^{z\mu}_V\right]-6\alpha\epsilon^{\mu\nu\rho\sigma}A^A_\nu F^V_{\rho\sigma}\,,\\
\tilde{J}^\mu_A(x) &= 4\kappa\lim_{z\to\infty}\left[\sqrt{-g}\mathcal{F}^{z\mu}_A\right]-2\alpha\epsilon^{\mu\nu\rho\sigma}A^A_\nu F^A_{\rho\sigma}\,.
\end{aligned} \tag{2.23}$$

The divergences of these currents are

$$\begin{aligned}
\partial_\mu\tilde{J}^\mu_V(x) &= 0\,,\\
\partial_\mu\tilde{J}^\mu_A(x) &= \frac{\alpha}{2}\epsilon^{\mu\nu\rho\sigma}\left[3F^V_{\mu\nu}F^V_{\rho\sigma}+F^A_{\mu\nu}F^A_{\rho\sigma}\right]\,,
\end{aligned} \tag{2.24}$$

where we used again the equations of motion (2.13). This clearly shows that the vector current is now conserved, while the anomaly is seen only in the axial sector. When the coefficient α is taken from string theory, the non-conservation of the axial current is exactly the same (including the numerical factor) as in QED coupled to external fermions [26]. In what follows we will work with these renormalised currents and action. We should also emphasise that when one considers chemical potential for a symmetry which is anomalous (as it is case here), just knowing the corrected action (2.20) may not be enough. Also, one has to be careful about the boundary conditions one has to impose on the states, as not all boundary conditions are allowed. We discuss these subtle issues in section 3.4.

2.4 The corrected Hamiltonian

The Lagrangian density of the action after inclusion of the anomaly counter term can be written as

$$\begin{aligned}\tilde{\mathcal{L}} = -\kappa\sqrt{-g}\left[\mathcal{F}_V^{0a}\mathcal{F}_{0a}^V + \frac{1}{2}\mathcal{F}_V^{ab}\mathcal{F}_{ab}^V + \mathcal{F}_A^{0a}\mathcal{F}_{0a}^A + \frac{1}{2}\mathcal{F}_A^{ab}\mathcal{F}_{ab}^A\right] \\ + \frac{\alpha}{4}\epsilon^{0abcd}\left[\mathcal{A}_0^A(3\mathcal{F}_{ab}^V\mathcal{F}_{cd}^V + \mathcal{F}_{ab}^A\mathcal{F}_{cd}^A) + 4\mathcal{A}_b^A(3\mathcal{F}_{0a}^V\mathcal{F}_{cd}^V + \mathcal{F}_{0a}^A\mathcal{F}_{cd}^A)\right]. \quad (2.25)\end{aligned}$$

The conjugate momenta associated with the vector and axial gauge fields thus take the form

$$\begin{aligned}\tilde{\Pi}_V^a &= \frac{\partial\tilde{L}}{\partial(\partial_0\mathcal{A}_a^V)} = \tilde{P}_V^{0a} = -2\kappa\sqrt{-g}\mathcal{F}_V^{0a} + 3\alpha\epsilon^{0abcd}\mathcal{A}_b^A\mathcal{F}_{cd}^V\,, \\ \tilde{\Pi}_A^a &= \frac{\partial\tilde{L}}{\partial(\partial_0\mathcal{A}_a^A)} = \tilde{P}_A^{0a} = -2\kappa\sqrt{-g}\mathcal{F}_A^{0a} + \alpha\epsilon^{0abcd}\mathcal{A}_b^A\mathcal{F}_{cd}^A\,.\end{aligned} \quad (2.26)$$

We then obtain the on-shell Hamiltonian as $\tilde{H} = \tilde{H}_{\text{Bulk}} + \tilde{H}_{\text{Bdy}}$, where the two contributions read

$$\begin{aligned}\tilde{H}_{\text{Bulk}} &= \kappa\int \mathrm{d}^3x\mathrm{d}z\sqrt{-g}\left[-\mathcal{F}_V^{0a}\mathcal{F}_{0a}^V + \frac{1}{2}\mathcal{F}_V^{ab}\mathcal{F}_{ab}^V - \mathcal{F}_A^{0a}\mathcal{F}_{0a}^A + \frac{1}{2}\mathcal{F}_A^{ab}\mathcal{F}_{ab}^A\right] \\ &= \kappa\int \mathrm{d}^3x\mathrm{d}z\sqrt{-g}\left[-\mathcal{F}^{0a}\mathcal{F}_{0a} + \frac{1}{2}\mathcal{F}^{ab}\mathcal{F}_{ab}\right],\end{aligned} \quad (2.27)$$

$$\tilde{H}_{\text{Bdy}} = \int \mathrm{d}^3x\mathrm{d}z\,\partial_a\left[\tilde{\Pi}_V^a\mathcal{A}_0^V + \tilde{\Pi}_A^a\mathcal{A}_0^A\right]. \quad (2.28)$$

Here we have used the gauge field equations (2.13) for the time component $\ell = 0$ (generalised Gauss law).

3 The spatially modulated phase

Having settled the issue of how to deal with the Chern-Simons term in the presence of external fields for the Sakai-Sugimoto model, we now want to find the ground state of the system, at strong coupling, in the presence of external magnetic field and non-vanishing axial and baryon chemical potentials. Based on the weak coupling, partonic, arguments which were mentioned in the introduction, we expect that the ground state should be a chiral magnetic spiral like configuration. In particular, we expect it to be *non-homogeneous*.

So far, for Sakai-Sugimoto model a non-homogeneous ground state was constructed in the presence of large enough axial chemical potential but with no external fields in [15] (at low temperature; see [27] for a high-temperature analysis). The main reason why such a state appeared was due to the nontrivial Chern-Simons term. We now want to see if this state persists and how it is modified once the external magnetic field is introduced.

3.1 Magnetic ground state ansatz in the presence of chemical potentials

We are interested in studying the ground state of the system at non-zero axial chemical potential μ_A and non-zero baryon chemical potential μ_B. In addition, we will turn on a constant magnetic field in the x^1 direction $\vec{B} = B\hat{x}_1$. The boundary conditions associated with this physical scenario are

$$\vec{\mathcal{A}}(z = \pm\infty) \;=\; \frac{1}{2}\vec{B} \times \vec{x}, \qquad \mathcal{A}_0(z = \pm\infty) = \mp\mu_A + \mu_B \,. \tag{3.1}$$

We will see that in fact our ansatz is insensitive to the baryon chemical potential, but we will keep it in the formulas for a little while longer.

Let us now consider our particular ansatz, in the gauge $\mathcal{A}_z = 0$. First, we want to introduce the vectorial and axial chemical potentials, hence we turn on $\mathcal{A}_0 = f(z)$ with the above boundary conditions. Second, we need to introduce the (constant) magnetic field in the boundary, hence we turn on a component of $\mathcal{A}$ transverse to the direction of $\vec{B}$: $\vec{\mathcal{A}}^T_B(x_2, x_3, z)$. In principle this function could depend on z, but the Bianchi identity tells us that in fact the magnetic field is *independent* of z. Therefore, we have for $\vec{\mathcal{A}}^T_B$

$$\vec{\mathcal{A}}^T_B(x_2, x_3) \;=\; \frac{1}{2}\vec{B} \times \vec{x} = \frac{B}{2}\left[-x_3\hat{x}_2 + x_2\hat{x}_3\right] . \tag{3.2}$$

Next by looking at the equations of motion for the $\vec{\mathcal{A}}^L_B$ component parallel to the magnetic field, we see that this component also has to be turned on, and is only a function of z,

$$\vec{\mathcal{A}}^L_B = a(z)\hat{x}_1 \,, \tag{3.3}$$

Finally, we expect that a chiral magnetic spiral will appear in the direction transverse to the external magnetic field

$$\vec{\mathcal{A}}^T_W(x_1, z) = h(z)\left[\cos(kx_1)\hat{x}_2 - \sin(kx_1)\hat{x}_3\right] , \tag{3.4}$$

i.e. it represents the chiral wave transverse to the boundary magnetic field satisfying

$$\nabla \times \vec{\mathcal{A}}^T_W \;=\; k\,\vec{\mathcal{A}}^T_W \,, \tag{3.5}$$

where $k = \pm|\vec{k}|$ and $\vec{k}$ is the spatial momentum. So in summary our ansatz is given by

$$\begin{aligned}
&\mathcal{A}^V_0 = f_V(z) \quad , \quad \mathcal{A}^A_0 = f_A(z)\,, \\
&\vec{\mathcal{A}}_V = \frac{B}{2}\left[-x_3\hat{x}_2 + x_2\hat{x}_3\right] + h_V(z)\left[\cos(kx_1)\hat{x}_2 - \sin(kx_1)\hat{x}_3\right] + a_V(z)\hat{x}_1 \,, \\
&\vec{\mathcal{A}}_A = a_A(z)\hat{x}_1 + h_A(z)\left[\cos(kx_1)\hat{x}_2 - \sin(kx_1)\hat{x}_3\right] ,
\end{aligned} \tag{3.6}$$

where the fields satisfy the boundary conditions

$$\begin{aligned} f_V(z \to \pm\infty) &= \mu_B\,, \qquad & f_A(z \pm \infty) &= \mp\mu_A\,, \\ h_V(z \to \pm\infty) &= 0 \quad , & h_A(z \to \pm\infty) &= 0\,, \\ a_V(z \to \pm\infty) &= 0 \quad , & a_A(z \to \pm\infty) &= \mp j\ . \end{aligned} \tag{3.7}$$

The Gauss law, i.e. the zeroth component of the equation of motion (2.13), is automatically satisfied for our ansatz. The remaining equations reduce, after integrating one of them with integration constant $\tilde{\rho}$, to

$$\sqrt{-g}\, g^{zz} g^{00} \partial_z f = 3\frac{\alpha}{\kappa}\left[Ba + \frac{k}{2}h^2\right] - \tilde{\rho}\,, \tag{3.8}$$

$$\partial_z\left[\sqrt{-g}\, g^{zz} g^{xx} \partial_z a\right] + 3\frac{\alpha}{\kappa} B \partial_z f = 0\,, \tag{3.9}$$

$$\partial_z\left[\sqrt{-g}\, g^{zz} g^{xx} (\partial_z h)\right] - \sqrt{-g}\,(g^{xx})^2 k^2 h + 3\frac{\alpha}{\kappa} k \partial_z f h = 0\,. \tag{3.10}$$

Restricting now to the metric (2.2), and substituting eq. (3.8) into (3.9) and (3.10) we obtain our master equations,

$$K_z \partial_z \hat{f} = -\hat{b} - \frac{1}{2}\hat{k}\hat{h}^2\,, \tag{3.11}$$

$$K_z \partial_z\left[K_z \partial_z \hat{b}\right] - \hat{B}^2\left[\hat{b} + \frac{1}{2}\hat{k}\hat{h}^2\right] = 0\,, \tag{3.12}$$

$$K_z \partial_z\left[K_z \partial_z \hat{h}\right] - K_z^{2/3}\hat{k}^2\hat{h} - \hat{k}\hat{h}\left[\hat{b} + \frac{1}{2}\hat{k}\hat{h}^2\right] = 0\,, \tag{3.13}$$

where

$$\hat{b} \equiv \hat{B}\hat{a} - \hat{\rho}\,, \tag{3.14}$$

and we have also introduced a set of dimensionless variables $\hat{f}$, $\hat{h}$, $\hat{a}$, $\hat{k}$, $\hat{\rho}$ and $\hat{B}$ defined by

$$f = \bar{\lambda}\, M_{\rm KK} \hat{f} \quad , \quad h = \bar{\lambda}\, M_{\rm KK}\, \hat{h} \quad , \quad a = \bar{\lambda}\, M_{\rm KK} \hat{a}\,, \tag{3.15}$$

$$k = M_{\rm KK}\hat{k} \quad , \quad \tilde{\rho} = \bar{\lambda}\, M_{\rm KK}^3\, \hat{\rho} \quad , \quad B = \bar{\lambda} M_{\rm KK}^2 \hat{B}\,, \tag{3.16}$$

with $\bar{\lambda} = \lambda/(27\pi)$. These coupled equations are in general not solvable analytically, except in the special case $k = 0$, which we will review next.

3.2 Review of the homogeneous solution

Before embarking on the full task of finding the non-homogeneous solutions to the equations of motion, we will in this section first review the homogeneous solution (i.e. the solution for which $k = 0$) in the presence of a constant magnetic field. This

is an abelian version of the solution first constructed in [8, 9], see also [17]. In the homogeneous case there is no transverse spiral, i.e. $h = 0$ and the equations of motion simplify to

$$\begin{aligned} \partial_{\tilde{z}} \hat{f} =& \hat{\rho} - \hat{B}\hat{a}\,, \\ \left(\partial_{\tilde{z}}^2 - \hat{B}^2\right)\hat{a} =& -\hat{B}\hat{\rho}\,, \end{aligned} \tag{3.17}$$

with $\tilde{z} = \arctan z$. These equations can be integrated exactly, and the solution takes the form

$$\begin{aligned} \hat{a}(z) &= \frac{\hat{C}_A}{\hat{B}}\cosh(\hat{B}\arctan z) + \frac{\hat{C}_B}{\hat{B}}\sinh(\hat{B}\arctan z) + \frac{\hat{\rho}}{\hat{B}}\,, \\ \hat{f}(z) &= -\frac{\hat{C}_A}{\hat{B}}\sinh(\hat{B}\arctan z) - \frac{\hat{C}_B}{\hat{B}}\cosh(\hat{B}\arctan z) + \hat{f}_0\,, \end{aligned} \tag{3.18}$$

where $\hat{C}_A, \hat{C}_B, \tilde{\rho}$ and $\hat{f}_0$ are four integration constants for the two second order differential equations. The corresponding field strengths take the form

$$\begin{aligned} \mathcal{F}_{z1} &= \frac{1}{1+z^2}\left[C_A\sinh(\hat{B}\arctan z) + C_B\cosh(\hat{B}\arctan z)\right]\,, \\ \mathcal{F}_{z0} &= -\frac{1}{1+z^2}\left[C_A\cosh(\hat{B}\arctan z) + C_B\sinh(\hat{B}\arctan z)\right]\,, \end{aligned} \tag{3.19}$$

and $C_{A/B} = \bar{\lambda} M_{KK} \hat{C}_{A/B}$. In terms of the baryonic and axial chemical potentials the boundary condition on $f(z)$ reads

$$f(z \to \pm\infty) = \mu_{L/R} = \mu_B \mp \mu_A\,. \tag{3.20}$$

From the expression for $f(z)$ these potentials are related to $\hat{C}_A$ and $\hat{C}_B$ by

$$\hat{C}_A = \frac{\hat{B}}{\sinh\left(\frac{\pi}{2}\hat{B}\right)}\hat{\mu}_A\,, \qquad \hat{C}_B = -\frac{\hat{B}}{\cosh\left(\frac{\pi}{2}\hat{B}\right)}(\hat{\mu}_B - \hat{f}_0)\,, \tag{3.21}$$

where $\mu_{A/B} = \bar{\lambda} M_{KK} \hat{\mu}_{A/B}$. In analogy with the analysis of [1] we are here interested in configurations in which there is a non-vanishing pion (or rather, η') gradient in the direction of the external field. Since we are working in the $\mathcal{A}_z = 0$ gauge, a pion field will appear as part of the axial, non-normalisable component of all $\mathcal{A}_\mu$'s (see [22, 23]). Hence, we impose the boundary condition[3]

$$a(z \to \pm\infty) = \mp j\,. \tag{3.22}$$

We should note here that this is not the most general boundary condition for the field $a(z)$, since we have set the even part to zero. Having thus reduced the parameter

[3]We stick to this notation, introduced in [17], but want to emphasise that even though using the symbol j suggests that the asymptotic value of a is a current, it is not.

space to the set $\{\mu_A, \mu_B, j\}$, we have the relations

$$\begin{aligned}
\hat{C}_A &= \frac{\hat{B}}{\sinh\left(\frac{\pi}{2}\hat{B}\right)}\hat{\mu}_A\,, \qquad \hat{\rho} = -\hat{B}\coth\left(\frac{\pi}{2}\hat{B}\right)\hat{\mu}_A\,, \\
\hat{C}_B &= -\frac{\hat{B}}{\sinh\left(\frac{\pi}{2}\hat{B}\right)}\hat{j}\,, \qquad \hat{f}_0 = \hat{\mu}_B - \coth\left(\frac{\pi}{2}\hat{B}\right)\hat{j}\,,
\end{aligned} \tag{3.23}$$

where $j = \bar{\lambda} M_{KK}\hat{j}$. Using these relations we can rewrite $\hat{f}(z)$ and $\hat{a}(z)$ as

$$\begin{aligned}
\hat{f}(z) &= \hat{\mu}_B - \hat{\mu}_A\frac{\sinh(\hat{B}\arctan z)}{\sinh\left(\frac{\pi}{2}\hat{B}\right)} + \hat{j}\left[\frac{\cosh(\hat{B}\arctan z)}{\sinh\left(\frac{\pi}{2}\hat{B}\right)} - \coth\left(\frac{\pi}{2}\hat{B}\right)\right]\,, \\
\hat{a}(z) &= \hat{\mu}_A\left[\frac{\cosh(\hat{B}\arctan z)}{\sinh\left(\frac{\pi}{2}\hat{B}\right)} - \coth\left(\frac{\pi}{2}\hat{B}\right)\right] - \hat{j}\frac{\sinh(\hat{B}\arctan z)}{\sinh\left(\frac{\pi}{2}\hat{B}\right)}\,.
\end{aligned} \tag{3.24}$$

Since the constant μ_B does not appear in the Hamiltonian, it is effectively a free parameter, which we are free to set to zero. As expected, we find that the baryon chemical potential has no effect on this abelian system. In contrast, minimising the Hamiltonian will impose a constraint on the axial chemical potential and j, as expected for physical systems.

In summary, we have two physical boundary values, μ_A and j, which are implicitly expressed in terms of the two parameters C_A and C_B. At any given fixed values of μ_A and j, we will want to compare the homogeneous solution given above to possible non-homogeneous condensates and determine which of the two has lower energy.

3.3 Currents for the homogeneous and non-homogeneous ansatz

The work of [17, 24], which studied the homogeneous solution discussed above, resulted in the interesting conclusion that there is *no* chiral magnetic effect present in the holographic Sakai-Sugimoto model. There are some subtleties with this which were pointed out in [16], to which we will return shortly. However, their result also leaves the open question as to whether there is a chiral magnetic effect for more general solutions to the equations of motion, for instance the non-homogeneous ones which we consider here.

So even before we find the full non-homogeneous solution, an important lesson might be learnt from an evaluation of the corrected holographic currents (2.23) for

the non-homogeneous ansatz. For our ansatz (3.6), the corrected currents become

$$\begin{aligned}
\tilde{J}^0_V &= -4\kappa \lim_{z\to\infty}\left[\sqrt{-g}g^{zz}g^{00}\partial_z f_V\right] - 12\alpha B j \\
&= -12\alpha \lim_{z\to\infty}\left[B a_A + k h_V h_A\right] - 12\alpha B j = 0\,, \\
\tilde{J}^1_V &= -4\kappa \lim_{z\to\infty}\left[\sqrt{-g}g^{zz}g^{xx}\partial_z a_V\right] + 12\alpha B \mu_A \\
&= 12\alpha B \lim_{z\to\infty} f_A + 12\alpha B\mu_A = 0\,, \\
\tilde{J}^2_V &= -4\kappa \lim_{z\to\infty}\left[\sqrt{-g}g^{zz}g^{xx}\partial_z \mathcal{A}^V_2\right] = -4\kappa M^2_{\rm KK} \lim_{z\to\infty}\left[K_z \partial_z h_V\right]\cos(kx_1)\,, \\
\tilde{J}^3_V &= -4\kappa \lim_{z\to\infty}\left[\sqrt{-g}g^{zz}g^{xx}\partial_z \mathcal{A}^V_3\right] = 4\kappa M^2_{\rm KK} \lim_{z\to\infty}\left[K_z \partial_z h_V\right]\sin(kx_1)\,, \\
\tilde{J}^0_A &= 4\kappa \lim_{z\to\infty}\left[\sqrt{-g}g^{zz}g^{00}\partial_z f_A\right] \\
&= \lim_{z\to\infty}\left[12\alpha\left(B a_V + \frac{k}{2}h_V^2 + \frac{k}{2}h_A^2\right) - 4\kappa\tilde{\rho}\right] = -4\kappa\tilde{\rho}\,, \\
\tilde{J}^1_A &= 4\kappa \lim_{z\to\infty}\left[\sqrt{-g}g^{zz}g^{xx}\partial_z a_A\right] = 4\kappa M^2_{\rm KK} \lim_{z\to\infty}\left[K_z \partial_z a_A\right]\,, \\
\tilde{J}^2_A &= 4\kappa \lim_{z\to\infty}\left[\sqrt{-g}g^{zz}g^{xx}\partial_z \mathcal{A}^A_2\right] = 4\kappa M^2_{\rm KK} \lim_{z\to\infty}\left[K_z \partial_z h_A\right]\cos(kx_1)\,, \\
\tilde{J}^3_A &= 4\kappa \lim_{z\to\infty}\left[\sqrt{-g}g^{zz}g^{xx}\partial_z \mathcal{A}^A_3\right] = -4\kappa M^2_{\rm KK} \lim_{z\to\infty}\left[K_z \partial_z h_A\right]\sin(kx_1)\,.
\end{aligned} \tag{3.25}$$

where we have used the gauge field equations for the components $\ell = 0$ and $\ell = 1$.

From (3.25) we see two important facts. First, the density of particles carrying baryonic charge is zero. This confirms once more that there is nothing baryonic in the solutions under consideration, in agreement with the fact that the baryon chemical potential μ_B decouples completely.

The second observation is that the component of the vector current *in the direction of the external magnetic field* is zero. This is in sharp contrast to what one would expect if there was a chiral magnetic effect present. We should, however, emphasise that it is possible to define corrected currents which are different from those above, if one decides to deal with the anomalous symmetry in a different way, see section 3.4. However, this alternative method, although it produces the chiral magnetic effect, suffers from other shortcomings, as we will explain.

The expressions (3.25) simplify further when we restrict to the homogeneous ansatz, for which one obtains

$$\begin{aligned}
&\tilde{J}^0_V = \tilde{J}^1_V = \tilde{J}^2_V = \tilde{J}^3_V = 0\,, \\
&\tilde{J}^0_A = 4\kappa M^2_{\rm KK}\tilde{B}\mu_A \coth(\frac{\pi}{2}\tilde{B}) = 12\alpha B\mu_A \coth(\frac{\pi}{2}\tilde{B})\,, \\
&\tilde{J}^1_A = -4\kappa M^2_{\rm KK}\tilde{B} j \coth(\frac{\pi}{2}\tilde{B}) = -12\alpha B(\mu_B - f_0)\,, \\
&\tilde{J}^2_A = \tilde{J}^3_A = 0\,.
\end{aligned} \tag{3.26}$$

We should emphasise once more that the vector (baryonic) currents vanish *only* when the contribution from the Bardeen term in the action is properly taken into account. One could in principle evaluate an "abelianised" version of the baryon number (second Chern class), $\sim \int F_{3z}F_{12}$. However, this expression is strictly speaking valid only in a *nonabelian* system, and in this situation one expects that the charge computed using the corrected conserved current $\tilde{J}^0_V$ should coincide with this topological number.

Our analysis shows that the fact that there is no chiral magnetic effect in the Sakai-Sugimoto model is not due to the simplified homogeneous ansatz, and that it is also not a consequence of the details of any numerical solution which we will present later; rather, the chiral magnetic effect is absent for the entire class of solutions captured by the ansatz (3.6). The contribution of the Bardeen terms required to make the vector currents conserved is crucial for the absence of the chiral magnetic effect.

We finally see that, in contrast to the homogeneous solution, where no vector currents are present at all, the non-homogeneous system exhibits transverse vector currents. This shows some resemblance to the chiral magnetic spiral of [28].

3.4 Chemical potentials for non-conserved charges

Given the rather convincing quasi-particle picture of the origin of the chiral magnetic effect at weak coupling [2, 3], it is somewhat surprising that it is not present in the model at hand at strong coupling. A reason for this discrepancy has been suggested in [16], in which it was emphasised that one should be careful in computing the effects of a chemical potential in theories for which the associated charge is not conserved.

The main observation made in [16] is that there are two ways to introduce a chemical potential into a thermal quantum system. One is to twist the fermions along the thermal circle, i.e. to impose

$$\Psi_{L,R}(\tau) = -e^{\pm\beta\mu_A}\Psi_{L,R}(\tau-\beta)\,, \tag{3.27}$$

instead of the usual anti-periodic boundary condition. This is what one would do at weak coupling. It was called the "B-formalism" in [16]. The other way is to keep anti-periodic boundary conditions, but instead use a shifted Hamiltonian,

$$\tilde{H} = H - \mu_A Q_L + \mu_A Q_R\,. \tag{3.28}$$

This coupling can be viewed as a coupling to a gauge field for which $\tilde{A}_0 = \mu_A$. We will refer to this as the "A-formalism" (in which we will temporarily put tildes on all objects, as above, for clarity). For a non-anomalous symmetry, these two formalisms are equivalent, and one can go from the B-formalism to the A-formalism using a gauge transformation involving the external gauge field, with parameter $\theta_A = -\mu_A t$, relating the gauge fields in the two formalisms according to

$$A_\mu = \tilde{A}_\mu + \partial_\mu\theta_A\,. \tag{3.29}$$

In terms of our holographic picture, this gauge transformation acts directly on the 5d gauge field, with a parameter $\Theta_A(z)$ that is z-dependent,

$$\Theta_A(z) = t g_A(z)\,, \qquad g_A(z \to \pm\infty) = \pm\mu_A\,. \tag{3.30}$$

which again acts on the gauge field as[4]

$$\mathcal{A}_m = \tilde{\mathcal{A}}_m + \partial_m \Theta_A\,. \tag{3.32}$$

The difference between the two formalism can thus be formulated in a clear holographic language as well: in the A-formalism the ansatz has $\tilde{\mathcal{A}}_0$ asymptoting to the chemical potential, whereas in the B-formalism the ansatz instead has this chemical potential stored in the $\mathcal{A}_z$ component. The chemical potential is then best written as

$$\mu_A = -\frac{1}{2}\int_{-\infty}^{\infty} \mathrm{d}z\, \mathcal{F}_{z0}\,, \tag{3.33}$$

which is nicely gauge invariant and independent of the formalism used.

This is all clear and unambiguous when the symmetry is non-anomalous. However, in the presence of an anomaly, one cannot pass from the formalism defined by (3.27) to that defined by (3.28). This is what happens in our system: as we discussed above, the 5d action after the anomaly correction (2.20) is not invariant under a chiral gauge transformation,

$$\begin{aligned}\tilde{S}[\tilde{\mathcal{A}}_\ell + \partial_\ell \Theta_A] = \tilde{S}[\tilde{\mathcal{A}}_\ell] + \frac{\alpha}{4}\epsilon^{\ell mnpq}\int \mathrm{d}^4x\mathrm{d}z\,(\partial_\ell\Theta_A)\left(3\tilde{\mathcal{F}}^V_{mn}\tilde{\mathcal{F}}^V_{pq} + \tilde{\mathcal{F}}^A_{mn}\tilde{\mathcal{F}}^A_{pq}\right)\\ =: \tilde{S}[\tilde{\mathcal{A}}_\ell] + \tilde{S}^\Theta[\tilde{\mathcal{A}}_\ell]\,.\end{aligned} \tag{3.34}$$

The anomaly implies that one of the two formalisms is incorrect.

The point of view of [16] is that there are strong indications that the B-formalism is the correct one in field theory. If one insists on computing with untwisted fermions, one needs to perform a gauge transformation, which not just introduces the chemical potential into A_0, but also modifies the action and Hamiltonian to correct for the fact that the action is not gauge invariant. To be precise, when one uses untwisted fermions, the action that one should use is the gauge-transformed action, which differs from the original one by the anomaly. This was called the "A'-formalism" (note the prime) in [16].

Let us see how this logic works for the Sakai-Sugimoto system under consideration here. The idea is thus that if we want to identify the chemical potential with

[4]The boundary gauge transformation parameter $\theta_A(x)$ is related to the 5d parameter by

$$\theta_A(x) \equiv \mp\Theta_A(x, z \to \pm\infty) = -\mu_A t\,, \tag{3.31}$$

with the perhaps somewhat inconvenient signs following from our relation between the bulk and boundary gauge fields (2.9).

the asymptotic value of $\tilde{\mathcal{A}}_0$, we should be working not with $\tilde{S}[\tilde{\mathcal{A}}_\ell]$ but rather with $\tilde{S}[\tilde{\mathcal{A}}_\ell] + \tilde{S}^\Theta[\tilde{\mathcal{A}}_\ell]$. In order to compute the currents, we need to compute the variation of the Θ_A, which takes the form

$$\delta S^{(\Theta_A)} = \alpha\epsilon^{m\ell npq}\int \mathrm{d}^4x\mathrm{d}z\,\partial_m\left[3(\partial_n\Theta_A)\tilde{\mathcal{F}}^V_{pq}\delta\tilde{\mathcal{A}}^V_\ell + (\partial_n\Theta_A)\tilde{\mathcal{F}}^A_{pq}\delta\tilde{\mathcal{A}}^A_\ell\right]. \tag{3.35}$$

The contribution of the Θ_A term to the holographic currents can be obtained using the dictionary

$$\Delta\tilde{J}^\mu_{V/A} = \pm\frac{\delta S^{(\Theta_A)}}{\delta\tilde{\mathcal{A}}^{V/A}_\mu(x, z=\infty)}\,, \tag{3.36}$$

We then obtain

$$\begin{aligned}\Delta\tilde{J}^\mu_V &= -6\alpha\epsilon^{\mu\nu\rho\sigma}(\partial_\nu\theta_A)\tilde{F}^V_{\rho\sigma} = 6\alpha\mu_A\epsilon^{\mu 0\rho\sigma}\tilde{F}^V_{\rho\sigma}\\ \Delta\tilde{J}^\mu_A &= -2\alpha\epsilon^{\mu\nu\rho\sigma}(\partial_\nu\theta_A)\tilde{F}^A_{\rho\sigma} = 2\alpha\mu_A\epsilon^{\mu 0\rho\sigma}\tilde{F}^A_{\rho\sigma}\,.\end{aligned} \tag{3.37}$$

These expressions are independent of the particular function $g_A(z)$ which one chooses in (3.30). For our ansatz (3.6) with the boundary conditions (3.7) we get

$$\begin{aligned}&\Delta\tilde{J}^0_V = 0\,,\\ &\Delta\tilde{J}^1_V = -12\alpha B\mu_A\,,\\ &\Delta\tilde{J}^2_V = \Delta\tilde{J}^3_V = 0\,,\\ &\Delta\tilde{J}^0_A = \Delta\tilde{J}^1_A = \Delta\tilde{J}^2_A = \Delta\tilde{J}^3_A = 0\,.\end{aligned} \tag{3.38}$$

This shows a very promising feature: any solution in this class will now exhibit the chiral magnetic effect, as there is a non-vanishing $\tilde{J}^1_V$ component.

Unfortunately, we will see later that things are more subtle at the level of the Hamiltonian. There are two main problems when writing down the A'-formalism for things more complicated than the currents. Firstly, any bulk quantities such as the Hamiltonian will typically depend on $g_A(z)$, not just on its asymptotic values. Secondly, it will turn out that even for a 'natural' choice of $g_A(z)$, for instance $g_A(z) = -f_A(z)$, the new Hamiltonian has the property that it does not lead to a minimum for non-homogeneous configurations. To see this requires some more details about this condensate, but let us here already present the expression for the corrected Hamiltonian. It can be written as

$$H_{\mathrm{Tot}}(\mathcal{A}_\ell, \Theta_A) = \tilde{H}_{\mathrm{Bulk}}(\mathcal{A}_\ell) + \tilde{H}_{\mathrm{Bdy}}(\mathcal{A}_\ell) + H^{(\Theta_A)}(\mathcal{A}_\ell, \Theta_A) \tag{3.39}$$

where $\tilde{H}_{\mathrm{Bulk}}(\mathcal{A}_\ell)$ and $\tilde{H}_{\mathrm{Bdy}}(\mathcal{A}_\ell)$ are given by (2.27), (2.28) and the Θ_A term is

$$\begin{aligned}H^{(\Theta_A)}(\mathcal{A}_\ell, \Theta_A) = \alpha\int \mathrm{d}^3x\mathrm{d}z\Big\{&\epsilon^{0abcd}(\partial_b\Theta_A)\left[3\mathcal{F}^V_{cd}(\partial_0\mathcal{A}^V_a) + \mathcal{F}^A_{cd}(\partial_0\mathcal{A}^A_a)\right]\\ &-\frac{1}{4}\epsilon^{\ell mnpq}(\partial_\ell\Theta_A)(3\mathcal{F}^V_{mn}\mathcal{F}^V_{pq} + \mathcal{F}^A_{mn}\mathcal{F}^A_{pq})\Big\}\end{aligned} \tag{3.40}$$

For our ansatz (3.6) with the boundary conditions (3.7) the theta term in the Hamiltonian take the form

$$\begin{aligned} H^{(\Theta_A)}(\mathcal{A}_\ell, \Theta_A) &= 2\alpha \int \mathrm{d}^3x\mathrm{d}z\, (\partial_0\Theta_A) \left[3B\partial_z a_V + \frac{k}{2}\partial_z(3h_V^2 + h_A^2)\right] \\ &= -\frac{2}{3}\mathcal{H}_0 \int \mathrm{d}z\, \partial_z\hat{g}_A \left[3\hat{B}\hat{a}_V + \frac{k}{2}(3h_V^2 + h_A^2)\right] \\ &= -\frac{2}{3}\mathcal{H}_0 \int \mathrm{d}z\, \partial_z\hat{g}_A \left[3(\hat{b}_V + \frac{k}{2}h_V^2) + \frac{k}{2}h_A^2\right] - 4\mathcal{H}_0\hat{\rho}\hat{\mu}_A\,. \end{aligned} \tag{3.41}$$

Specialising to $g_A(z) = -f_A(z)$ we get

$$H^{(\Theta_A)}(\mathcal{A}_\ell, \Theta_A) = -\frac{2}{3}\mathcal{H}_0 \int \mathrm{d}z\, \frac{1}{K_z} \left[\hat{b}_V + \frac{\hat{k}}{2}\hat{h}_V^2 + \frac{\hat{k}}{2}\hat{h}_A^2\right] \left[3(\hat{b}_V + \frac{k}{2}h_V^2) + \frac{k}{2}h_A^2\right] - 4\mathcal{H}_0\hat{\rho}\hat{\mu}_A\,. \tag{3.42}$$

In the homogeneous case we get

$$H^{(\Theta_A)}(\mathcal{A}_\ell, \Theta_A) = -\mathcal{H}_0\hat{C}_A^2 \left[\frac{\sinh(\pi\hat{B})}{\hat{B}} + \pi\right] - 4\mathcal{H}_0\hat{\rho}\hat{\mu}_A\,. \tag{3.43}$$

This boundary term can have drastic consequences for the phase structure of the theory: we will see in section 3.6 that it disfavours non-homogeneous configurations.

We should emphasise that the procedure for introducing the A'-formalism in the holographic context is, unfortunately, rather ambiguous. This is essentially because the required boundary condition on the gauge transformation parameter $\Theta_A(z)$, given in (3.31), does not uniquely specify the behaviour of $\Theta_A(z)$ in the bulk. In contrast, this kind of ambiguity does not appear in field theory, as gauge transformation which untwists fermions, and "moves" chemical potential into temporal component of the gauge potential, is unique.

Instead of using the A'-formalism one could consider doing the holographic computation directly in the B-formalism. This would require writing the solution in the $A_0 = 0$ gauge (the fermions are not directly accessible so it is unclear whether additional changes are required to implement the twisting). This does lead to a CME, but the Hamiltonian again turns out to have no minimum for non-homogeneous configurations. Some details are given in appendix A.2.

3.5 Perturbative stability analysis of the homogeneous solution

In this section we will perturbatively analyse the stability of the homogeneous solution (3.24), in order to show that this configuration is unstable and wants to "decay" to a non-homogeneous solution (3.6) (whose explicit form will be found later). Our

analysis here is a revision of the work done in [11], but our findings differ from theirs in an important way which is crucial for the remainder of our paper.

Our starting point is given by the equations of motion linearised around the configuration (3.24). Following [11], we will look for fluctuations of the modes transverse to the direction of the external field, i.e. along (A_1, A_2), since these should lead to the formation of a chiral spiral. These fluctuations are given by

$$\delta A_i = \delta A_i(\omega, k) e^{-i\omega t + ikx_1} \qquad (i = 2, 3)\,. \tag{3.44}$$

The equations of motion for the fluctuations $(\delta A_1, \delta A_2)$ are coupled, but they diagonalise in the complex basis

$$\delta A^{(\pm)} \equiv \delta A_2 \pm i\delta A_3\,, \tag{3.45}$$

where the equations become

$$K_z^{-1/3}(\omega^2 - k^2)\delta A^{(\pm)} + M_{\rm KK}^2 \partial_z (K_z \partial_z \delta A^{(\pm)}) \pm \frac{N_c}{8\pi^2\kappa}(k\mathcal{F}_{0z} + \omega\mathcal{F}_{1z})\delta A^{(\pm)} = 0\,. \tag{3.46}$$

Here $\mathcal{F}_{1z}, \mathcal{F}_{0z}$ are field strengths of the background homogeneous solution (3.19), and we will express all results in terms of the constants C_A and C_B (instead of μ_A and j) in order enable a simpler comparison with the results of [11].

Given values of C_A and C_B, we numerically solve equation (3.46). As usual in perturbation theory, solutions with real ω represent fluctuations that are stable, while those for which ω has a positive imaginary part correspond to instabilities, since they are exponentially growing in time. Fluctuations for which $\omega = 0$ are marginal and have to be analysed in the full nonlinear theory in order to see if they correspond to unstable directions in configuration space. We will argue now that, while [11] has correctly identified the perturbatively unstable solutions with complex ω, they have missed the marginally unstable modes, which are actually unstable in the full theory. In the following section we will then explicitly construct the new vacua corresponding to these marginal modes.

Before presenting solutions to the equation (3.46), observe that this equation exhibits the symmetry $t \to -t, \omega \to -\omega$, which means that all solutions will come in pairs $(\omega, -\omega)$. Additionally, when solving this equation, one looks for *normalisable* solutions, i.e. one looks for the solutions that behave as $\delta A^{(\pm)} \sim 1/z$ near the boundaries.

Let us start by discussing the solutions with only C_A non-vanishing. At $B = 0$ these correspond to solutions with $j = 0$. Samples of these solutions are shown in figure 1. We see that as $|C_A|$ is increased, the two branches of solutions come closer to the $\omega = 0$ axis and then touch (the middle plot in figure 1). For all those values of $|C_A|$, given any momenta k, there is always real ω solution. However, as $|C_A|$ is increased even more, the two branches of solutions separate along the k-axis, so that

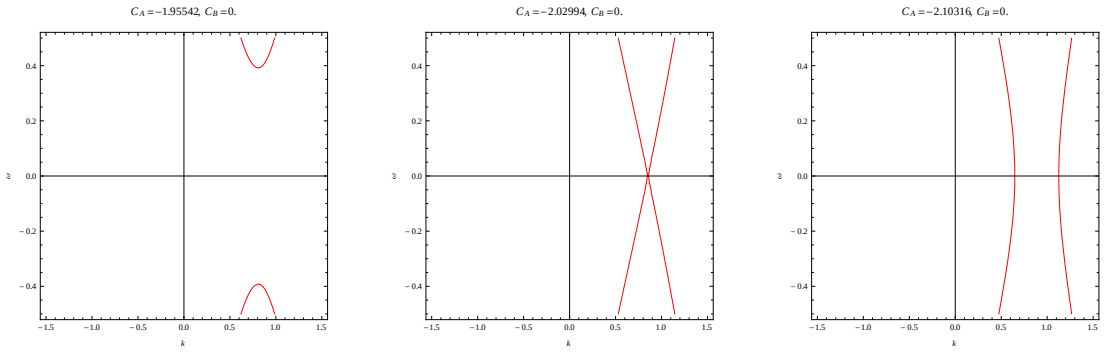

Figure 1. Dispersion relation for small fluctuations at vanishing C_B and increasing values of C_A. In the last plot, the region between the two $\omega = 0$ modes corresponds to modes with positive imaginary ω, hence signalling proper instability. This follows Kim et al. [11].

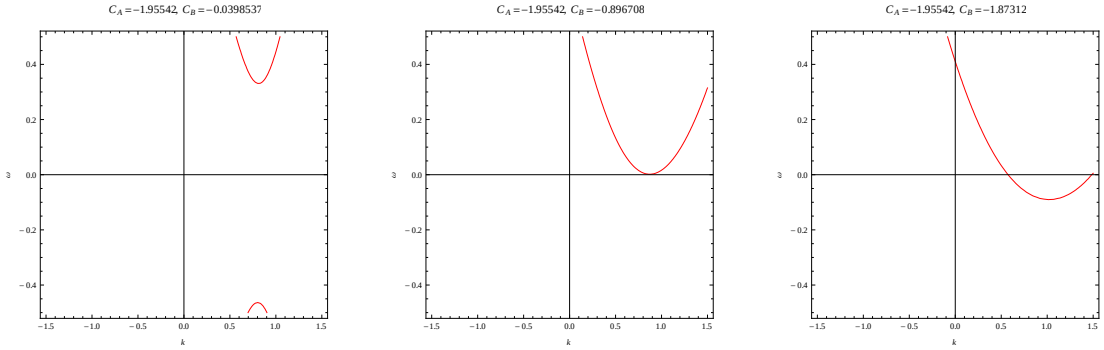

Figure 2. Dispersion relation at fixed value of C_A and increasing values of C_B. Modes with $\omega = 0$ occur for sufficiently large C_B, but in the region on the $\omega = 0$ axis between these two roots, there are no strictly unstable modes. Nevertheless, the ω could signal that there appears a new ground state.

there is a region of momenta for which there are no real ω solutions (see the third plot of figure 1). For these "forbidden" values of the momenta, one can explicitly find solutions with complex ω, which clearly signal a proper instability of the solution. These modes have previously been found in [11].

Let us now turn on $|C_B|$, while keeping $|C_A|$ fixed. Samples of these solutions are shown in figure 2. We see that as $|C_B|$ is increased, the two branches of solutions shift in the vertical direction, while the distance between them remains non-vanishing (which is the reason why this other branch is not visible in the second and third plots). For some value of $|C_B|$, the upper branch crosses the $\omega = 0$ axis, and continues to go towards negative ω. We thus see that for large enough $|C_B|$, marginal $\omega = 0$ modes are always present in the spectrum. In the next section, we will show that these modes, which were previously missed in the literature, are actually unstable once non-linearities are taken into account.

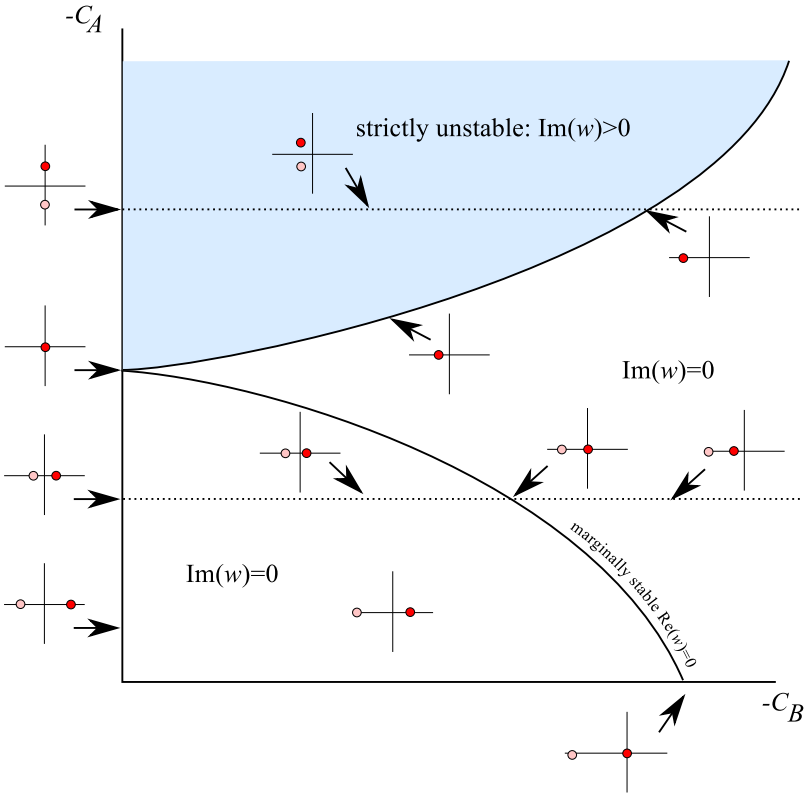

Figure 3. The physical picture (not to scale) that arises from the analysis of the dispersion relation. The plot displays the location of the physical modes at the extrema of the curves in figures 1 and 2, but now depicted in the complex ω plane.

These findings are summarised in figure 3. Depicted there is the behaviour of the frequencies ω of the fluctuation modes at the 'extrema' of the dispersion relation plots, as a function of the two parameters C_A and C_B. For a generic value of C_B and $C_A = 0$, one root is always positive. As C_A is increased from zero, the positive root (red dot) moves towards the left, until it becomes zero. This defines the lower, solid curve of marginal modes in figure 3. Above this curve there is always a marginally stable mode in the spectrum, and thus potentially an instability. As C_A is increased further, both roots eventually develop a positive imaginary part, and we enter the region of strictly unstable modes (the blue shaded region). This area was previously discussed in [11].[5]

[5] As we have already mentioned before, we disagree with their interpretation of C_B being related to the baryon chemical potential; see also below.

3.6 The inhomogeneous solutions to the equations of motion

Having established the location of the unstable and marginally stable modes in the fluctuation spectrum of the homogeneous solution, we would now like to explicitly construct the non-homogeneous solutions to which they are expected to decay, and study their properties. In our previous work [15] we have explicitly constructed a non-homogeneous solution in the presence of non-vanishing *axial* chemical potential, and in the absence of a magnetic field. We will therefore first discuss solutions with nonzero μ_A and non-zero B, which are a natural generalisation of those considered before. We will then introduce a non-zero potential j as well and discuss how the solutions behave as a function of this parameter.

The upshot of our previous analysis [15] was that for large enough axial chemical potential, larger than some critical value, a non-homogeneous solution is formed. The relation between the chemical potential and axial particle density was almost linear, similar to the homogeneous case. However, a particular density of particles was achieved for a smaller value of the chemical potential than in the homogeneous configuration. The wave number characterising the period of the non-homogeneous solution turned out to be very weakly sensitive to the actual value of the particle charge density in the canonical ensemble (or to the value of the chemical potential in the case of the grand canonical ensemble). The first things we would like to know is whether any of these characteristics change in the presence of an external magnetic field.

Our starting point is the nonlinear system of equations (3.11), (3.12) and (3.13). We first observe that the function $\hat{f}(z)$ appears only in the first equation (3.11), and this equation can be directly integrated once we determine the functions $\hat{b}(z)$ and $\hat{h}(z)$, from the other two equations.

Hence, we first need to solve equations (3.12) and (3.13). The parameters $\hat{B}$ and $\hat{k}$ in these equations correspond to the external magnetic field and the momentum of the transverse spiral, and are fixed at this stage. There are then four undetermined constants corresponding to non-normalisable and normalisable modes for each of the functions $\hat{b}$ and $\hat{h}$. However, we solve equations (3.12), (3.13) requiring that the transverse spiral describes a normalisable mode,

$$\hat{h}(z) = \frac{h_0}{z} + \cdots , \tag{3.47}$$

i.e. we impose that the only external field is the magnetic field, and that there are no transverse external fields.

In contrast, the function $\hat{b}(z)$ (or alternatively, $\hat{a}(z)$, see (3.14)), which describes the longitudinal field, does have a non-normalisable component. For example, on the positive side of the U-shaped brane it generically behaves as

$$\hat{b}(z) = b_0 + \frac{b_1}{z} + \cdots \quad (z \to \infty) , \tag{3.48}$$

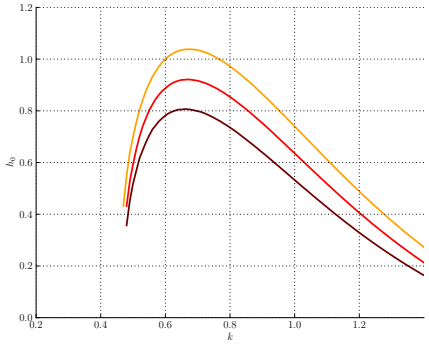

Figure 4. Value of h_0 versus k at fixed $B = 1.0$, for increasing values of $|C_B|$. Increasing $|C_B|$ makes the curve go up, indicating that a full new non-linear ground state exists for increasing $|C_B|$ and decreasing $|C_A|$. That is to say, the $\omega = 0$ fluctuation modes are the indicators of the transition to a new ground state, not the $\mathrm{Im}(\omega) > 0$ modes.

where the coefficients b_0 and b_1 are given by

$$\begin{aligned} b_0 &= C_A \cosh\left(\frac{\pi B}{2}\right) + C_B \sinh\left(\frac{\pi B}{2}\right) , \\ b_1 &= BC_B \cosh\left(\frac{\pi B}{2}\right) - BC_A \sinh\left(\frac{\pi B}{2}\right) . \end{aligned} \tag{3.49}$$

However, just like for the homogeneous solution, this non-normalisable component of the solution corresponds to a gradient of the η' field and not to an external field (we will provide more evidence of this in section 3.6). Its unusual appearance as a non-normalisable mode is a consequence of our choice of the $A_z = 0$ gauge.

We should note that at this stage we do not impose that $\hat{b}$ or $\hat{h}$ are of definite parity. We numerically solve the equation of motion using the shooting method, and to do this we only need to specify three undetermined constants h_0, C_A and C_B on one side of the U-shaped brane, as well as the parameter B and k in the equations. We solve equations for various values of constants and parameters, but keep only those for which $\hat{h}$ is normalisable.

A first indication of the behaviour of the solutions can be obtained by looking at the effect of increasing C_B at non-zero value of B. Remember from section 3.5 that there exists a marginally stable mode in the spectrum, which follows the downward bending curve in figure 3. Along this curve there might be a decay to a new ground state. That this indeed happens is easily confirmed by looking for nonlinear solutions at non-zero C_A and C_B. A number of physical solutions is depicted in figure 4. They confirm that the marginal modes found in the previous section in fact correspond to true instabilities and new ground states. However, these figures say little about the actual physics, as neither C_A nor C_B are physical parameters.

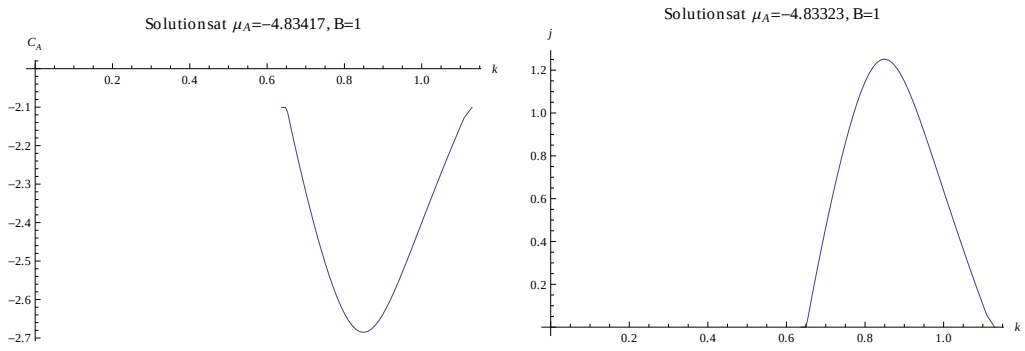

Figure 5. Data for solutions at $C_B = 0$, for the (arbitrary) value $\mu = -4.83$. The second plot clearly shows that when $B \neq 0$, constant j solutions require a scan through the full parameter space $\{h_0, k, C_A, C_B\}$.

It is tempting to associate C_B with a baryon chemical potential, but as we have already mentioned, this is incorrect, as the parameter μ_B completely decouples and does not influence the value of the Hamiltonian. Instead, the correct interpretation is that the physical parameters in our problem are μ_A and j, which happen to be related in a non-trivial way to C_A and C_B. Families of solutions (parametrised by k) at fixed μ_A and j lie on curves in the space spanned by C_A and C_B, which only become straight lines at $C_B = 0$ when $B = 0$. This is once more clearly visible in figure 5. This depicts a family of solutions at constant μ_A, parametrised by k, at $C_B = 0$. These clearly do not have a constant value of j.

In order to find solutions with both μ_A and j fixed, we need to allow for a variation of both C_A and C_B as a function of k. Even with the magnetic field fixed to a particular value, this still means that the normalisable solutions lie on a curve in a four-dimensional parameter space spanned by $\{h_0, k, C_A, C_B\}$. This makes a brute force scan computationally infeasible. Independent of the large dimensionality of this problem, we also found that the larger μ_A cases require substantial computational time because of the fact that the asymptotic value $h(-\infty)$ varies rather strongly as a function of k and the other parameters. In other words, the valley of solutions is rather steep and the bottom of the valley, where $h(z)$ is normalisable at $z \to -\infty$, is difficult to trace. In this respect, it is useful to note that a solution written in C++ using odeint [29] and GSL [30] outperformed our Mathematica implementations by two to three orders of magnitude (!) in these computations. The details of the procedure which we followed can be found in appendix A.3.

We first focus on solutions at fixed and rather arbitrary value $B = 1$; the dependence on B will be discussed in the next section. We will mainly discuss $j = 0$ solutions. Our numerical investigations of $j \neq 0$ solutions show that all of these ac-

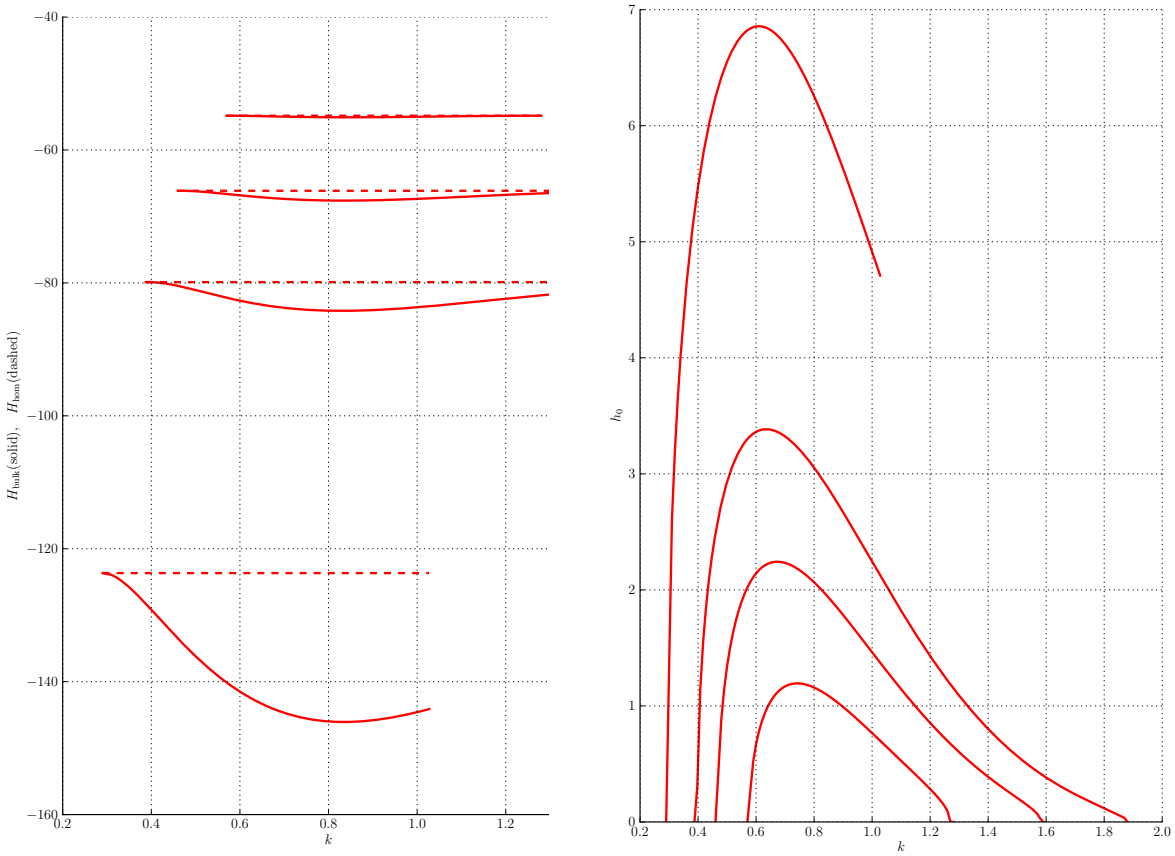

Figure 6. Left: Comparison of the energy of the non-homogeneous ground state (solid curve) with the energy of the homogeneous state (dashed curves) for $j = 0, B = 1$ and four values of μ_A; from top to bottom $\mu_A = -5.5, -6.0, -6.5$ and -7.5. Right: h_0 versus k, for the same values of the parameters (from bottom to top).

tually have higher free energy, and are thus not real ground states of the system (see below). In figure 6 we display a set of configurations at constant μ_A and vanishing j. Also depicted is the difference of the Hamiltonian of the homogeneous solution for this pair of μ_A, j values, and the Hamiltonian of the non-homogeneous solution.

As in earlier work without magnetic field [15, 27], there is a family of solutions parametrised by the wave momentum k, and the physical solution is the one for which the Hamiltonian is minimised. Perhaps somewhat surprisingly, for smaller values of the chemical potential (we have done computations up to about $\mu_A = -8$) the momentum $k_{\rm g.s.}$ at which the non-homogeneous ground state attains its minimum energy is only very weakly dependent on μ_A. Our numerics for the range of μ_A up to -7.5 show that the ground state momentum for all these cases equals 0.83 to within less than one percent. Furthermore, this ground state momentum is also the same (to within numerical accuracy) as the ground state momentum for the $B = 0$ case

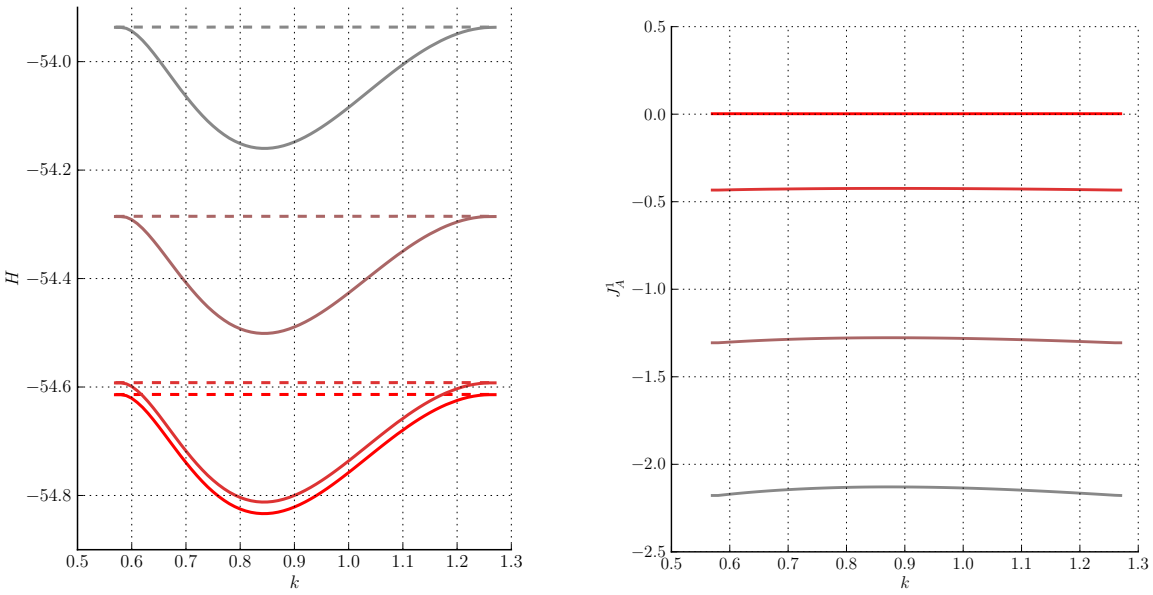

Figure 7. The dependence of the Hamiltonian and the current J^1_A on the parameter j (showing $j = 0$, 0.1, 0.3 and 0.5 bottom to top on the left, top to bottom on the right). This shows that minimisation with respect to j drives the system to $j = 0$, both for the homogeneous and for the non-homogeneous state, and that this also drives the η'-gradient sitting in J^1_A to zero. Under $j \to -j$ the Hamiltonian is invariant while J^1_A changes sign.

analysed in [15]. This is despite the fact that the actual solutions are quite different. It would be interesting to understand this behaviour better.

If one evaluates the Hamiltonian of the A'-formalism (3.42), one finds that all non-homogeneous configurations always have higher energy than the corresponding homogeneous one at the same values of μ_A and j. We take this as a strong sign that there is still something un-understood about the A'-formalism, as the analysis of section 3.5 clearly indicates a perturbative instability. It is in principle possible that we are not looking at the correct ansatz for the ground state, but we consider this unlikely. A similar statements holds for the B-formalism.

The dependence of these solutions on j can also be computed, and is depicted in figure 7. From those plots one observes two things. Firstly, a minimisation of the Hamiltonian with respect to j drives the system to $j = 0$. Secondly, a non-zero j leads to a non-vanishing J^1_A current, which can be interpreted as an η'-gradient. Together, these observations show that the preferred non-homogeneous state is one with a vanishing η'-gradient.

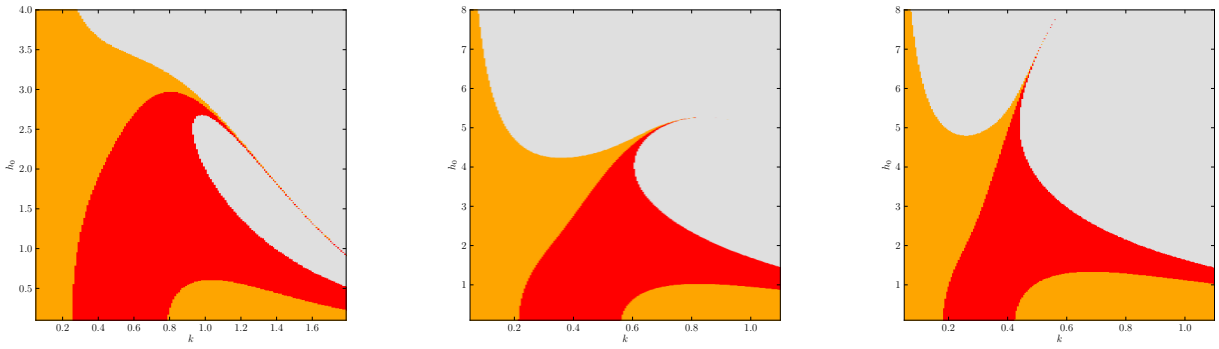

Figure 8. The sign of $h(z \to -\infty)$, where red and orange regions denote minus and plus respectively, and grey regions correspond to solutions that diverge when $z \to -\infty$. Normalisable non-homogeneous solutions sit at the boundary between red and orange regions. The branch that starts near $k = 0.2$ is the relevant one, as it has the lowest energy. It becomes increasingly difficult to find numerically as it is sandwiched in a steep valley as k increases. All plots are at $C_A = -2.4$, with $B = 1.9$, 2.1 and 2.3 respectively. Note the different axis scales on the first plot.

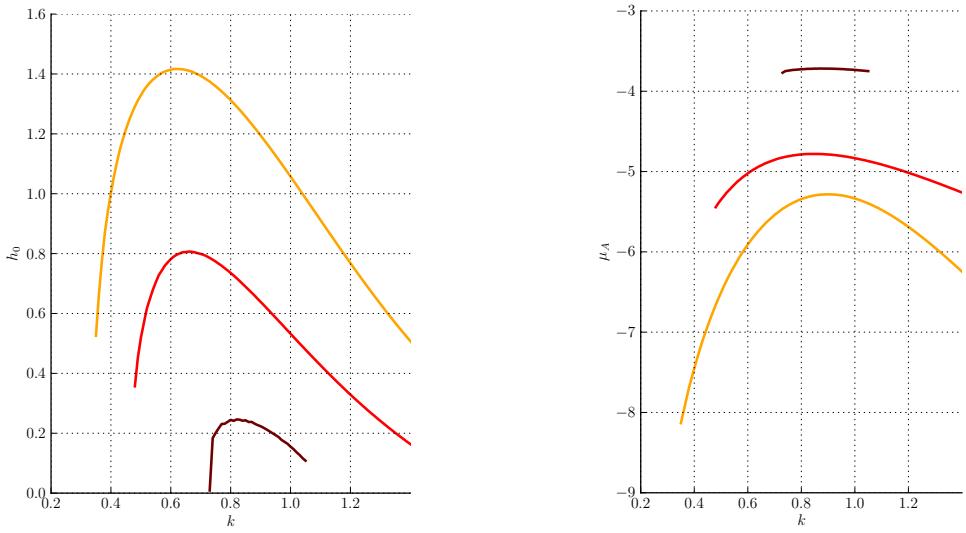

Figure 9. Left: The increase of B from 0 to 1.0 to 1.5 (bottom black to top orange curves) at $C_B = 0$ and fixed $C_A = -2.4$ has the effect of raising the curves of normalisable solutions. This implies that a larger magnetic field requires a smaller value of $|C_A|$ to trigger an instability. Right: However, one cannot conclude anything about the effect at constant μ_A from this, since this physical parameter varies over the curves in the figure on the left.

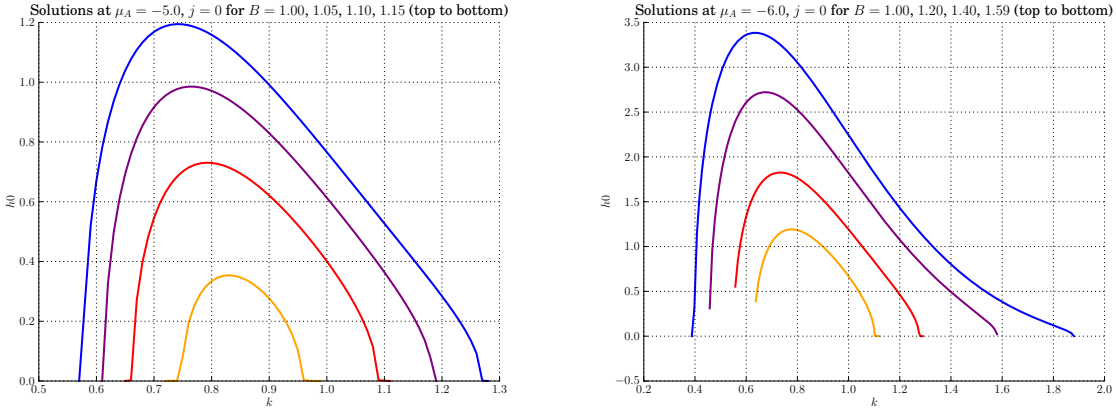

Figure 10. Solutions at constant $\mu = -5.0$ (left) and $\mu = -6.0$ (right) and $j = 0$, for various values of the magnetic field. This shows that a magnetic field *suppresses* the instability to a non-homogeneous ground state, and there is a critical magnetic field $B_{\text{crit}}(\mu_A)$ above which the non-homogeneous solution ceases to exist.

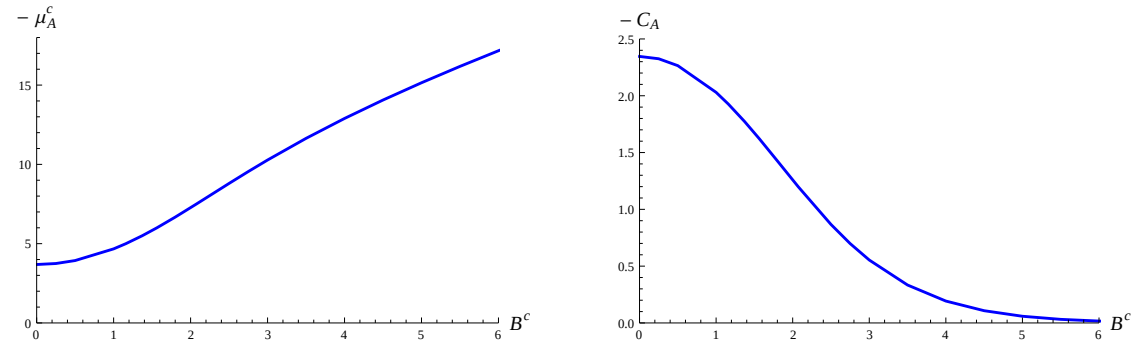

Figure 11. Results from a linearised analysis close to the critical magnetic field. Left: critical chemical potential (i.e. the potential for which a non-homogeneous ground state first develops) versus critical magnetic field (i.e. the field for which the solution disappears). Right: as determined earlier for the non-linear case, the parameter C_A goes to zero (asymptotically) as B increases.

3.7 Critical magnetic field

For larger magnitudes of the external magnetic field, the numerics becomes increasingly expensive as the valleys of solutions to the equations of motion rapidly become steeper and are more and more closely approached by regions in parameter space in which no regular solutions exist (i.e. regions in which $h(z \to \infty)$ diverges). See figure 8 for an impression.

A first analysis which one can make is to simply scan for normalisable solutions at fixed C_A and C_B, for increasing values of B. This leads to plots like in figure 9.

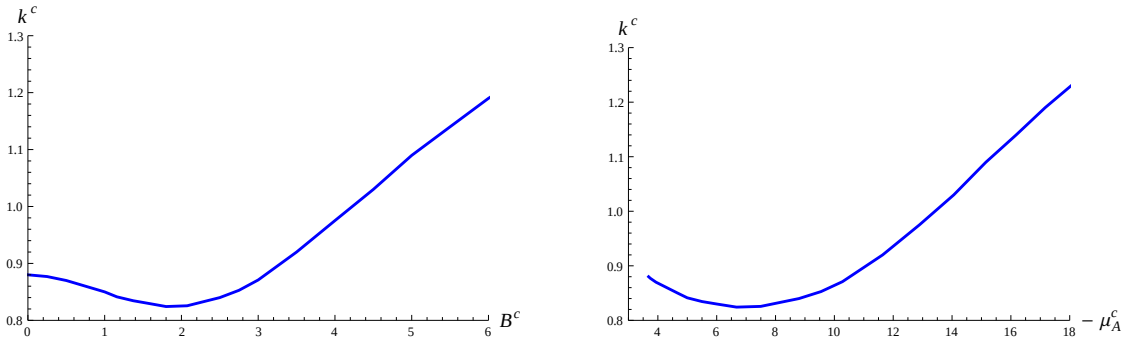

Figure 12. Dependence of the ground state momentum $k_{\text{g.s.}}$ of the critical solution on the magnetic field or the chemical potential, computed in the linear approximation. The non-linear solutions which we computed cover the regime up to about $B_c = 2$. One should keep in mind that the linear approximation will break down for sufficiently large values of B_c.

One observes that a larger magnetic field requires a smaller $|C_A|$ for the chiral spiral solution to exist. In [11] this effect was seen at the level of the perturbative instability analysis, and led the authors to conclude that a magnetic field enhances the instability. However, this conclusion is premature and actually incorrect. What one needs to do is to analyse the effect of the magnetic field on solutions at fixed value of μ_A and j, not at fixed values of the unphysical parameters C_A and C_B.

If one does this more elaborate analysis, the conclusion is actually opposite: the magnetic field tends to stabilise the homogeneous solution, and there exists a critical $B_{\text{crit}}(\mu_A)$ above which the non-homogeneous solution ceases to exist. This can be seen in figure 10, where solutions at fixed μ_A and j are depicted. By increasing B sufficiently slowly while keeping the other physical parameters fixed, we can determine this B_{crit} in numerical form.

It is difficult to get a good picture of B_{crit} versus μ_A, as the numerics become expensive, for reasons we have mentioned earlier. However, we can make use of the fact that near the critical magnetic field, the parameter h_0 is small. Assuming that this implies that the entire function $h(z)$ is small, we can then use a linear approximation to the equations of motion, which is much easier to solve. The result of this linear analysis is depicted in figures 11 and 12. The latter shows that the ground state momentum $k_{\text{g.s.}}$ is actually not as flat as the non-linear computations suggests.

For larger B, one should keep in mind that the results may be invalidated for a variety of reasons. Firstly, the linear approximation may break down, as smallness of h_0 does not necessarily imply smallness of the full function $h(z)$. Secondly, we have seen that the valley near the non-linear solutions becomes very steep for large values of B, and hence the linear solution may deviate quite strongly from the non-linear

one for large B. Thirdly, when B is large, DBI corrections to the equations of motion may become relevant, as higher powers of the field strength are no longer necessarily small. For these reasons, one should be careful interpreting the large B_c regime of figure 12.

4 Conclusions and open questions

We have analysed in detail the instability of the Sakai-Sugimoto model in the presence of a chiral chemical potential μ_A, an η'-gradient j and a magnetic field B. We have shown that the presence of marginally stable modes (overlooked in [11]) is a signal for decay towards a non-homogeneous chiral spiral like ground state. Minimising the Hamiltonian on a constant μ_A, constant j curve leads to a unique ground state momentum $k_{\text{g.s.}}$ (see figure 6), which for small B is only weakly dependent on μ_A. Increasing the magnetic field to sufficiently large values suppresses the instability and drives the system back to the homogeneous phase (figure 12). This result may be related to the effective reduction of the Landau levels in a strong magnetic field (see [31]).

A linear analysis suggests that the ground state momentum may have a non-trivial dependence on the chemical potential, and might be compatible with a linear scaling at large μ_A (as in the Deryagin-Grigoriev-Rubakov non-homogeneous large-N_c QCD ground state [32]). However, substantial additional work is necessary to determine whether this is indeed happening in the full non-linear theory.

We have found that a recent proposal for the correction of the currents [13, 16], while capable of producing the chiral magnetic effect both in the homogeneous and non-homogeneous ground states, is incomplete. It is a) not unique and b) leads to a Hamiltonian which does not prefer the non-homogeneous ground state. We emphasise that this is a problem with the currents and boundary terms in the Hamiltonian, as the perturbative instability analysis is not affected by these corrections, and neither are the non-linear solutions.

Acknowledgments

We thank Karl Landsteiner for discussions about [13, 16]. This work was partially supported by STFC grant ST/G000433/1. The work of MZ was supported by an EPSRC Leadership Fellowship.

A Appendix: Technical details

A.1 The Hamiltonian after the anomaly corrections

Here we will give a detailed derivation of the Hamiltonian for the Sakai-Sugimoto system taking special care about surface terms that are present, as well as taking into account the corrections to the action coming from the anomaly.

After anomaly in the system have been corrected by inclusion of extra terms in the action, the full Langrangian density can be written as

$$\begin{aligned}\tilde{\mathcal{L}} = -\kappa\sqrt{-g}\left[\mathcal{F}_V^{0a}\mathcal{F}_{0a}^V + \frac{1}{2}\mathcal{F}_V^{ab}\mathcal{F}_{ab}^V + \mathcal{F}_A^{0a}\mathcal{F}_{0a}^A + \frac{1}{2}\mathcal{F}_A^{ab}\mathcal{F}_{ab}^A\right] \\ + \frac{\alpha}{4}\epsilon^{0abcd}\Big[\mathcal{A}_0^A(3\mathcal{F}_{ab}^V\mathcal{F}_{cd}^V + \mathcal{F}_{ab}^A\mathcal{F}_{cd}^A) + 4\mathcal{A}_b^A(3\mathcal{F}_{0a}^V\mathcal{F}_{cd}^V + \mathcal{F}_{0a}^A\mathcal{F}_{cd}^A)\Big]\,. \quad \text{(A.1)}\end{aligned}$$

The conjugate momenta associated with the vector and axial gauge fields take the form

$$\begin{aligned}\tilde{\Pi}_V^a &= \frac{\partial\tilde{L}}{\partial(\partial_0\mathcal{A}_a^V)} = -2\kappa\sqrt{-g}\mathcal{F}_V^{0a} + 3\alpha\epsilon^{0abcd}\mathcal{A}_b^A\mathcal{F}_{cd}^V\,, \\ \tilde{\Pi}_A^a &= \frac{\partial\tilde{L}}{\partial(\partial_0\mathcal{A}_a^A)} = -2\kappa\sqrt{-g}\mathcal{F}_A^{0a} + \alpha\epsilon^{0abcd}\mathcal{A}_b^A\mathcal{F}_{cd}^A\,.\end{aligned} \quad \text{(A.2)}$$

Hence, the on-shell Hamiltonian takes the form $\tilde{H} = \tilde{H}_{\text{Bulk}} + \tilde{H}_{\text{Bdy}}$

$$\tilde{H}_{\text{Bulk}} = \kappa\int \mathrm{d}^3x\mathrm{d}z\sqrt{-g}\left[-\mathcal{F}^{0a}\mathcal{F}_{0a} + \frac{1}{2}\mathcal{F}^{ab}\mathcal{F}_{ab}\right] \quad \text{(A.3)}$$

$$\tilde{H}_{\text{Bdy}} = \int \mathrm{d}^3x\mathrm{d}z\,\partial_a\left[\tilde{\Pi}_V^a\mathcal{A}_0^V + \tilde{\Pi}_A^a\mathcal{A}_0^A\right]\,. \quad \text{(A.4)}$$

where we have used the gauge field equations for the time component of gauge potential (generalised Gauss law).

For our inhomogeneous ansatz the conjugate momenta simplify to

$$\begin{aligned}\tilde{\Pi}_V^z &= 2\kappa\sqrt{-g}g^{zz}g^{00}\partial_z f_V - 6\alpha(a_A B + k h_A h_V) = 0\ , \\ \vec{\tilde{\Pi}}_V &= -6\alpha\left[a_A(\partial_z h_V) - h_A(\partial_z a_V)\right]\left[\sin(kx_1)\hat{x}_2 + \cos(kx_1)\hat{x}_3\right]\ , \\ \tilde{\Pi}_A^z &= 2\kappa\sqrt{-g}g^{zz}g^{00}\partial_z f_A - 2\alpha k h_A^2 = 6\alpha B a_V + 3\alpha k h_V^2 + \alpha k h_A^2 - 2\kappa\tilde{\rho}\,, \\ \vec{\tilde{\Pi}}_A &= -2\alpha\left[a_A(\partial_z h_A) - h_A(\partial_z a_A)\right]\left[\sin(kx_1)\hat{x}_2 + \cos(kx_1)\hat{x}_3\right]\ .\end{aligned} \quad \text{(A.5)}$$

Using this result and the boundary conditions we have imposed on the fields, one gets the boundary term of the Hamiltonian

$$\tilde{H}_{\text{Bdy}} = -2\kappa\tilde{\rho}\int \mathrm{d}^3x\mathrm{d}z\partial_z f_A = 4\kappa V_x\tilde{\rho}\mu_A = -V_x\tilde{J}_A^0\mu_A\,. \quad \text{(A.6)}$$

The bulk term simplifies for our ansatz to

$$\tilde{H}_{\rm Bulk} = \kappa \int {\rm d}^3x{\rm d}z \Big\{ -\sqrt{-g}g^{zz}g^{00}(\partial_z f)^2 + \sqrt{-g}g^{zz}g^{xx}\left[(\partial_z h)^2 + (\partial_z a)^2\right] \tag{A.7}$$

$$+ \sqrt{-g}(g^{xx})^2\left[B^2 + k^2h^2\right]\Big\}\,. \tag{A.8}$$

In terms of the variables (3.16) the bulk and boundary terms take the form

$$\tilde{H}_{\rm Bulk} = \mathcal{H}_0 \int {\rm d}z \Big\{ \frac{1}{K_z}\left[\hat{b} + \frac{\hat{\alpha}}{2}\hat{k}\hat{h}^2\right]^2 + K_z\left[(\partial_z\hat{h})^2 + \left(\frac{\partial_z\hat{b}}{\hat{\alpha}\hat{B}}\right)^2\right] \tag{A.9}$$

$$+ K_z^{-1/3}\hat{k}^2\hat{h}^2\Big\} + \tilde{H}_{\rm Div}\,, \tag{A.10}$$

$$\tilde{H}_{\rm Bdy} = 4\mathcal{H}_0\hat{\rho}\hat{\mu}_A\,, \tag{A.11}$$

where $\mathcal{H}_0 = M_{\rm KK}^4 V_x \bar{\lambda}^3 N_c/(8\pi^2)$, $\hat{b} = \hat{B}\hat{a} - \hat{\rho}$ and $H_{\rm Div} = \mathcal{H}_0\hat{B}^2\int {\rm d}z\, K_z^{-1/3}$. For the homogeneous case we get simple analytic result

$$\begin{aligned}\tilde{H}_{\rm Bulk} &= 2\mathcal{H}_0\hat{B}\coth(\frac{\pi}{2}\hat{B})(\hat{\mu}_A^2 + \hat{j}^2) + \tilde{H}_{\rm Div} \\ &= \mathcal{H}_0(\hat{C}_A^2 + \hat{C}_B^2)\frac{\sinh(\hat{B}\pi)}{\hat{B}} + \tilde{H}_{\rm Div}\,,\end{aligned} \tag{A.12}$$

$$\tilde{H}_{\rm Bdy} = -4\mathcal{H}_0\hat{B}\coth(\frac{\pi}{2}\hat{B})\hat{\mu}_A^2 = -2\mathcal{H}_0\hat{C}_A^2\frac{\sinh(\hat{B}\pi)}{\hat{B}}\,. \tag{A.13}$$

A.2 The B-formalism ansatz

In formalism B the time component of the chiral gauge field is zero at the boundary. An ansatz that preserves the field strengths (and hence the equations of motion) is given by

$$\begin{aligned}&\mathcal{A}_z^V = -t\,\partial_z f_V \quad , \quad \mathcal{A}_z^A = -t\,\partial_z f_A\,, \\ &\mathcal{A}_0^V = 0 \quad , \quad \mathcal{A}_0^A = 0\,, \\ &\vec{\mathcal{A}}_V = \frac{B}{2}\left[-x_3\hat{x}_2 + x_2\hat{x}_3\right] + h_V(z)\left[\cos(kx_1)\hat{x}_2 - \sin(kx_1)\hat{x}_3\right] + a_V(z)\hat{x}_1\,, \\ &\vec{\mathcal{A}}_A = a_A(z)\hat{x}_1 + h_A(z)\left[\cos(kx_1)\hat{x}_2 - \sin(kx_1)\hat{x}_3\right]\,,\end{aligned} \tag{A.14}$$

which should be used together with the boundary conditions

$$\begin{aligned}&\mathcal{A}_z^V(z\to\pm\infty) = \mathcal{A}_z^A(z\to\pm\infty) = 0\,, \\ &h_V(z\to\pm\infty) = h_A(z\to\pm\infty) = 0\,, \\ &a_V(z\to\pm\infty) = a_A(z\to\pm\infty) = \mp j\,.\end{aligned} \tag{A.15}$$

The components of the vector and axial currents take the same form as those in the A-formalism, given in (3.25), with the exception of $\tilde{J}^1_V$ which reads

$$\tilde{J}^1_V = -4\kappa \lim_{z\to\infty} \left[\sqrt{-g} g^{zz} g^{xx} \partial_z a_V\right] = 12\alpha B \lim_{z\to\infty} f_A = -12\alpha B \mu_A \,. \tag{A.16}$$

This in particular implies that there is a non-zero chiral magnetic effect in formalism B.

A.3 Scanning parameter space for solutions

We recall from the main text that we aim for the minimisation of the Hamiltonian as a function of the condensate momentum k, on curves which have fixed values of μ_A and j. Unfortunately, the latter two parameters are determined only indirectly, after a solution has been found; their dependence on the shooting parameters h_0, C_A and C_B is not known analytically. Minimising the Hamiltonian over curves at fixed value of C_A and C_B would in general not be equivalent (i.e. wrong).

One could in principle make a fine-grained lattice scan for solutions in the parameter space spanned by $\{h_0, k, C_A, C_B\}$, and then consider only those points which have a certain fixed value of μ_A and j. This, however, is computationally extremely expensive, and wastes a lot of time on regions of parameter space which will never be used. We therefore follow a different approach.

The general problem which we need to solve for an efficient determination of the required curves is the following. We have a d-dimensional parameter space of configurations, and physical solutions are those in which $d-1$ functions of the configuration are vanishing simultaneously. One of these functions is always the value of the function $h(z)$ evaluated at $-\infty$, as this imposes normalisability. Among the other functions we have, for instance, the value of μ_A for this configuration minus some fixed reference value, in case we want to scan for solutions at this fixed value of the chemical potential. This 'isocurve tracing' problem is most easily implemented by starting from one known point on which the functions are simultaneously zero, and then using a version of the Newton-Raphson method to find the location of a neighbouring simultaneous zero.[6] If we have n lattice points in every direction of parameter space, this brings the computational cost down from being order $O(n^d)$ to the much more tractable $O(n)$.

We start by scanning for physical solutions at $C_B = 0$ and some fixed value of C_A, which is a two-dimensional problem in $\{h_0, k\}$ space and yields curves like those in figure 5. On these curves neither μ_A nor j will in general be constant. However, one can choose one point on such a solution curve, and use this as a seed point p^{seed} for the isocurve tracing described above. Denoting the value of μ_A and j by μ_A^{seed} and j^{seed} respectively, we then trace the common zero of the three functions $h(-\infty)$,

[6] General purpose Mathematica and C++ implementations of this isocurve tracing algorithm are available upon request from the authors.

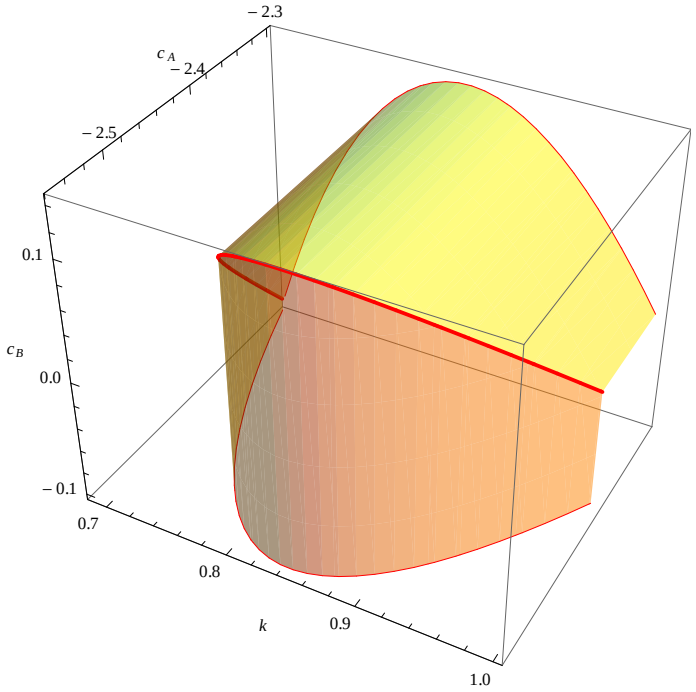

Figure 13. Typical curve of solutions, here at constant $\mu_A = -4.83$ and constant $j = 0.64$ (thick curve) and for $B = 1$. The orange/yellow surfaces show the projections onto the $\{k, C_A\}$ and $\{k, C_B\}$ planes respectively. Only for vanishing magnetic does this curve lie completely inside the $\{k, C_A\}$ plane.

$\mu_A - \mu_A^{\text{seed}}$ and $j - j^{\text{seed}}$ in the four-dimensional parameter space $\{h_0, k, C_A, C_B\}$ (only when $B = 0$ do these curves lie completely in the $\{h_0, k, C_A\}$ subspace). A typical solution is depicted in figure 13. The only remaining problem with these curves is now that in general $j^{\text{seed}} \neq 0$ (the only such points on the curves in figure 5 are located on the endpoints of those curves, where the coefficient h_0 goes to zero).

In order to find curves at $j = 0$, we start again from p^{seed}, but first do an isocurve trace at fixed k in the $\{h_0, C_A, C_B\}$ space until we find a point at which $j = 0$. An example is given in figure 14. This point is then used as our new seed point $\tilde{p}^{\text{seed}}$ for the four-dimensional scan. Repeating the whole process using a seed point obtained for different initial values of C_A then produces a set of curves at $j = 0$ for various constant values of μ_A.

On each of these curves we can now finally compute the Hamiltonian as a function of k, and find the value k_{min} for which it is minimised. For a sample set of values of μ_A the result is depicted in figure 6.

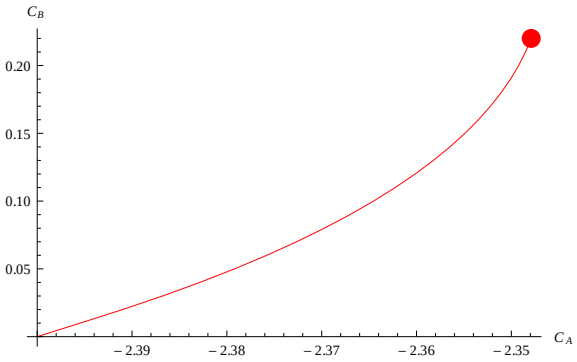

Figure 14. Typical isocurve trace, here at the sample value of $\mu_A = -4.83$, starting from the seed point p^{seed} with $C_B = 0$ to the new seed point $\tilde{p}^{\text{seed}}$ (indicated by the dot) at which $j = 0$ and both C_A and C_B are non-zero.

References

[1] D. T. Son and M. A. Stephanov, "Axial anomaly and magnetism of nuclear and quark matter", *Phys. Rev.* **D77** (2008) 014021, arXiv:0710.1084.

[2] D. E. Kharzeev, L. D. McLerran, and H. J. Warringa, "The Effects of topological charge change in heavy ion collisions: 'Event by event P and CP violation'", *Nucl. Phys.* **A803** (2008) 227–253, arXiv:0711.0950.

[3] K. Fukushima, D. E. Kharzeev, and H. J. Warringa, "The Chiral Magnetic Effect", *Phys. Rev.* **D78** (2008) 074033, arXiv:0808.3382.

[4] D. Son and A. R. Zhitnitsky, "Quantum anomalies in dense matter", *Phys. Rev.* **D70** (2004) 074018, arXiv:hep-ph/0405216.

[5] M. A. Metlitski and A. R. Zhitnitsky, "Anomalous axion interactions and topological currents in dense matter", *Phys. Rev.* **D72** (2005) 045011, arXiv:hep-ph/0505072.

[6] D. T. Son and P. Surowka, "Hydrodynamics with triangle anomalies", *Phys. Rev. Lett.* **103** (2009) 191601, arXiv:0906.5044.

[7] D. E. Kharzeev and H.-U. Yee, "Chiral Magnetic Wave", *Phys. Rev.* **D83** (2011) 085007, arXiv:1012.6026.

[8] O. Bergman, G. Lifschytz, and M. Lippert, "Magnetic properties of dense holographic QCD", *Phys. Rev.* **D79** (2009) 105024, arXiv:0806.0366.

[9] E. G. Thompson and D. T. Son, "Magnetized baryonic matter in holographic QCD", *Phys. Rev.* **D78** (2008) 066007, arXiv:0806.0367.

[10] O. Bergman, J. Erdmenger, and G. Lifschytz, "A review of magnetic phenomena in probe-brane holographic matter", arXiv:1207.5953.

[11] K.-Y. Kim, B. Sahoo, and H.-U. Yee, "Holographic chiral magnetic spiral", *JHEP* **10** (2010) 005, arXiv:1007.1985.

[12] C. Hoyos, T. Nishioka, and A. O'Bannon, "A Chiral Magnetic Effect from AdS/CFT with Flavor", *JHEP* **1110** (2011) 084, arXiv:1106.4030.

[13] A. Gynther, K. Landsteiner, F. Pena-Benitez, and A. Rebhan, "Holographic anomalous conductivities and the chiral magnetic effect", *JHEP* **1102** (2011) 110, arXiv:1005.2587.

[14] O. Aharony, K. Peeters, J. Sonnenschein, and M. Zamaklar, "Rho meson condensation at finite isospin chemical potential in a holographic model for QCD", *JHEP* **082** (2007) 1007, arXiv:0709.3948.

[15] C. B. Bayona, K. Peeters, and M. Zamaklar, "A non-homogeneous ground state of the low-temperature Sakai-Sugimoto model", *JHEP* **1106** (2011) 092, arXiv:1104.2291.

[16] K. Landsteiner, E. Megias, L. Melgar, and F. Pena-Benitez, "Gravitational anomaly and hydrodynamics", *J.Phys.Conf.Ser.* **343** (2012) 012073, arXiv:1111.2823.

[17] A. Rebhan, A. Schmitt, and S. A. Stricker, "Anomalies and the chiral magnetic effect in the Sakai-Sugimoto model", *JHEP* **1001** (2010) 026, arXiv:0909.4782.

[18] A. Yamamoto, "Chiral Magnetic Effect on the lattice", arXiv:1207.0375.

[19] K. Fukushima and K. Mameda, "Wess-Zumino-Witten action and photons from the Chiral Magnetic Effect", arXiv:1206.3128.

[20] A. Gorsky, P. Kopnin, and A. Zayakin, "On the Chiral Magnetic Effect in soft-wall AdS/QCD", *Phys. Rev.* **D83** (2011) 014023, arXiv:1003.2293.

[21] V. Rubakov, "On chiral magnetic effect and holography", arXiv:1005.1888.

[22] T. Sakai and S. Sugimoto, "Low energy hadron physics in holographic QCD", *Prog. Theor. Phys.* **113** (2005) 843–882, hep-th/0412141.

[23] T. Sakai and S. Sugimoto, "More on a holographic dual of QCD", *Prog. Theor. Phys.* **114** (2006) 1083–1118, hep-th/0507073.

[24] A. Rebhan, A. Schmitt, and S. Stricker, "Holographic chiral currents in a magnetic field", *Prog.Theor.Phys.Suppl.* **186** (2010) 463–470, arXiv:1007.2494.

[25] W. A. Bardeen, "Anomalous Ward identities in spinor field theories", *Phys. Rev.* **184** (1969) 1848–1857.

[26] M. Peskin and D. Schroeder, "An introduction to quantum field theory", Perseus, 1995.

[27] H. Ooguri and C.-S. Park, "Spatially modulated phase in holographic quark-gluon plasma", *Phys. Rev. Lett.* **106** (2011) 061601, arXiv:1011.4144.

[28] G. Basar, G. V. Dunne, and D. E. Kharzeev, "Chiral Magnetic Spiral", *Phys.Rev.Lett.* **104** (2010) 232301, arXiv:1003.3464.

[29] K. Ahnert and M. Mulansky, "Odeint - solving ordinary differential equations in C++", arXiv:1110.3397, http://www.odeint.com.

[30] M. G. et al., "GNU Scientific Library Reference Manual, 3rd edition", 2009.

[31] G. Basar and G. V. Dunne, "The Chiral Magnetic Effect and axial anomalies", arXiv:1207.4199.

[32] D. V. Deryagin, D. Y. Grigoriev, and V. A. Rubakov, "Standing wave ground state in high density, zero temperature QCD at large-N_c", *Int. J. Mod. Phys.* **A7** (1992) 659–681.